

UNITED NATIONS EDUCATIONAL, SCIENTIFIC AND CULTURAL ORGANIZATION  
**INTERNATIONAL CENTRE FOR THEORETICAL PHYSICS**  
I.C.T.P., P.O. BOX 586, 34100 TRIESTE, ITALY, CABLE: CENTRATOM TRIESTE



UNITED NATIONS INDUSTRIAL DEVELOPMENT ORGANIZATION



## **INTERNATIONAL CENTRE FOR SCIENCE AND HIGH TECHNOLOGY**

c/o INTERNATIONAL CENTRE FOR THEORETICAL PHYSICS 34100 TRIESTE (ITALY) VIA GRIGNANO, 9 (ADRIATICO PALACE) P.O. BOX 586 TELEPHONE 040-224572 TELEFAX 040-224573 TELEX 460449 APH I

SMR/760-50

### **"College on Atmospheric Boundary Layer and Air Pollution Modelling" 16 May - 3 June 1994**

**"Review of Modelling of Atmospheric Diffusion  
& Dispersion of Pollutants"**

and

**"LIDAR"**

T. MIKKELSEN  
Department of Meteorology  
Risø National Laboratory  
Roskilde, Denmark

***Please note: These notes are intended for internal distribution only.***

College on Atmospheric Boundary Layer  
and Air Pollution Modelling.

MAY 16 - June 3  
1994

Lectures by Torben Mikkelsen

Dep. of Meteorology & Wind Energy  
Risø National Laboratory  
P.O. Box 49, DK - 4000 Roskilde, DENMARK

Lecture 1. Tuesday May 24 11.00-12.00

- Review of Modelling of  
Atmospheric diffusion and  
dispersion of Pollutants.

Lecture 2.  
C & LIDAR

Wednesday May 25. 11.00-12.00

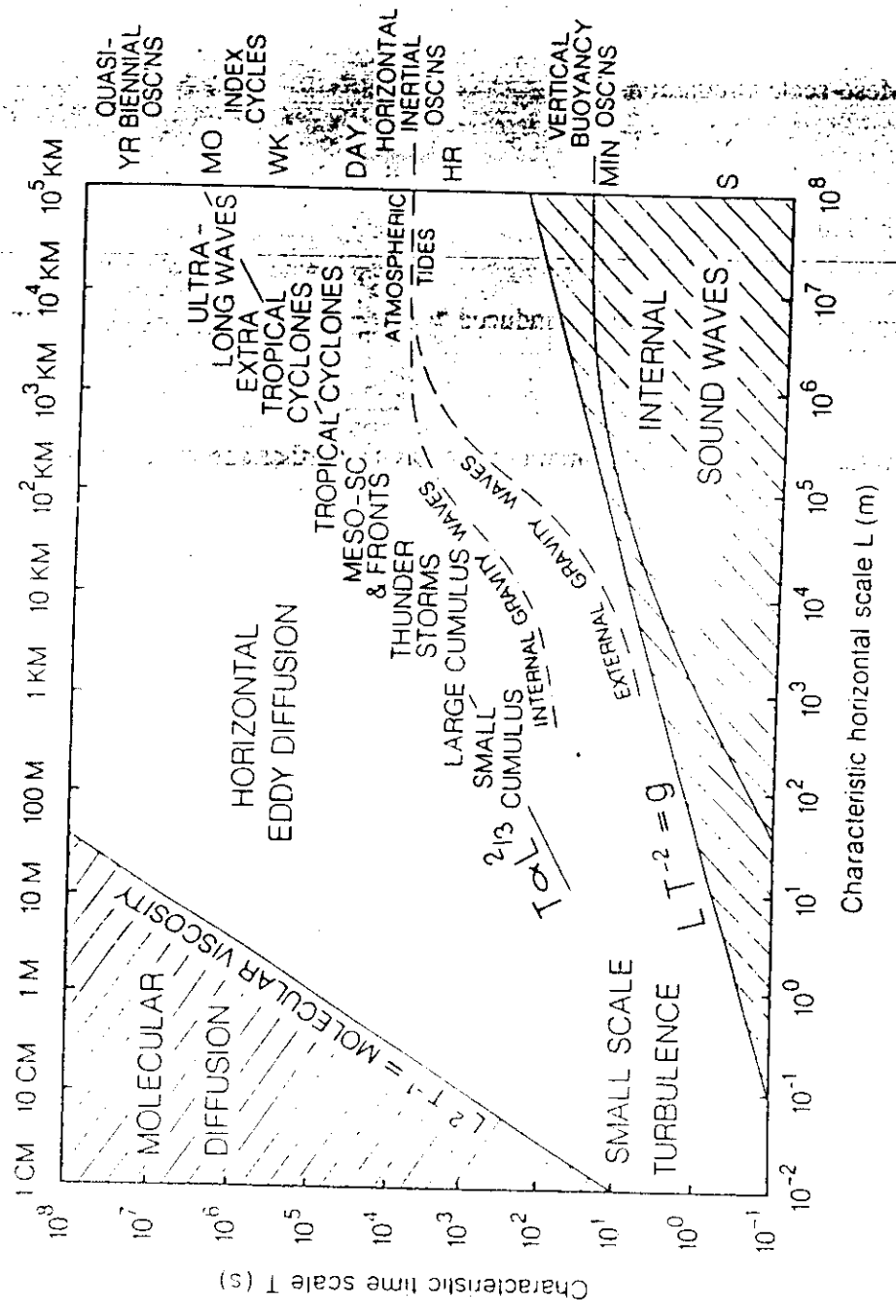


Fig. 1 Spatial and temporal characteristics of atmospheric phenomena (after Smagorinsky 1981).

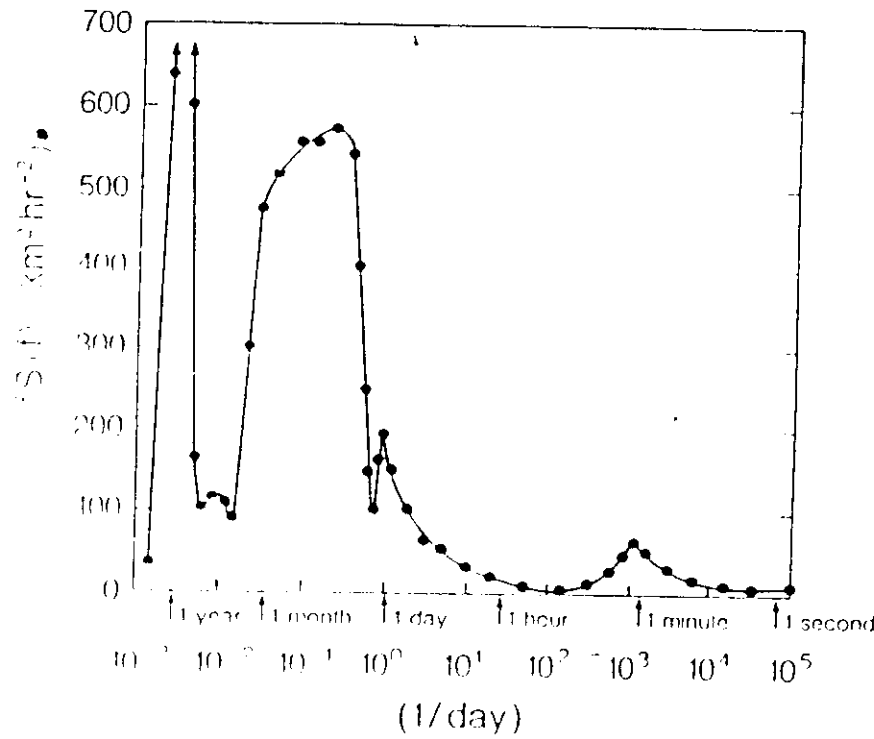


Fig. 2. Spectral density  $S_f$  of the zonal wind component in the free atmosphere (after Vinnichenko 1970).

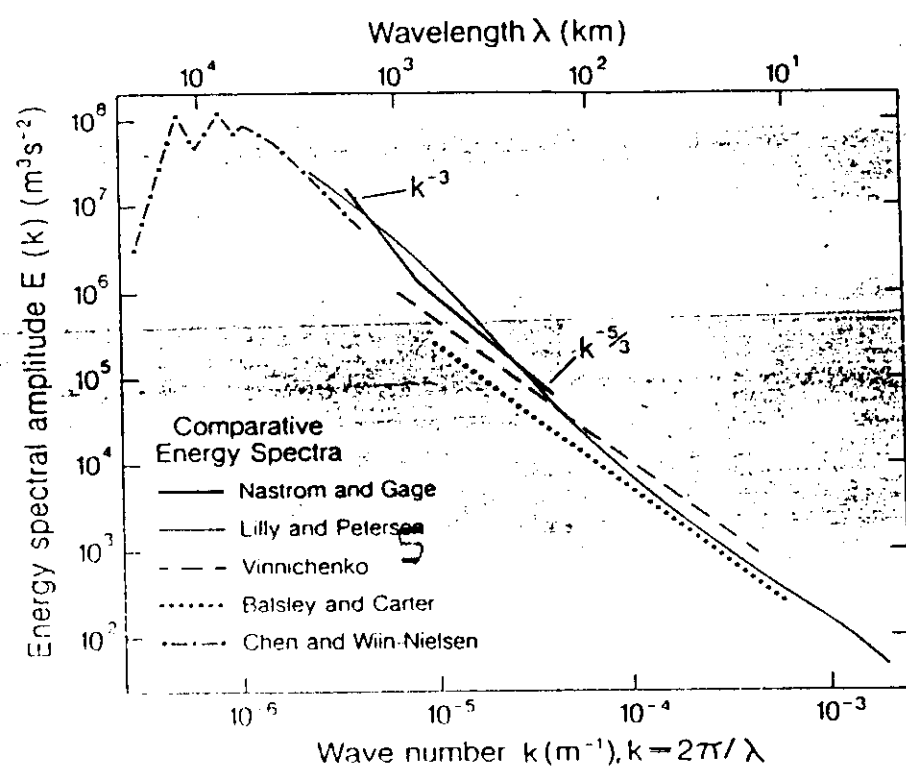
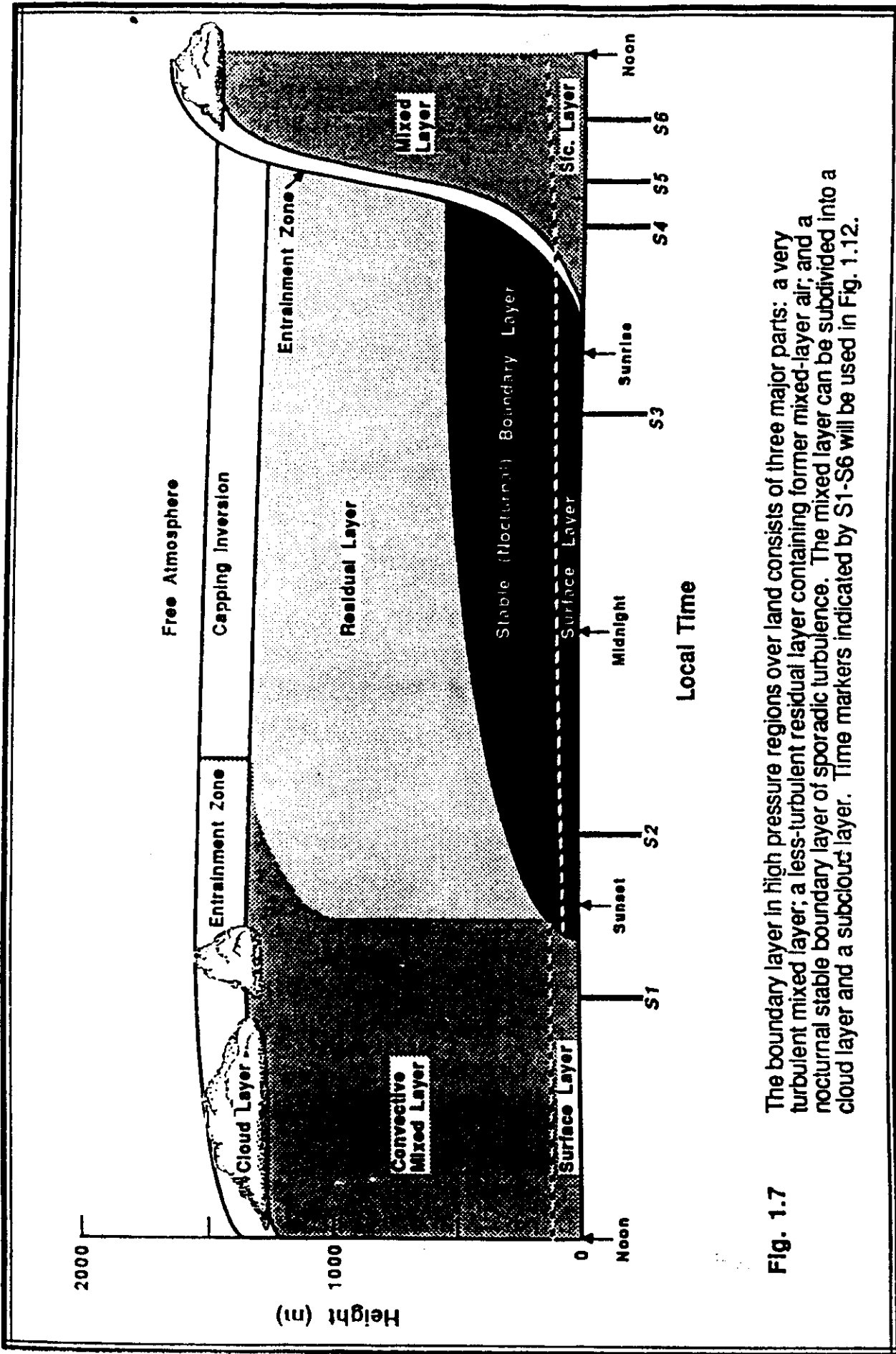


Fig. 3. Line spectra of horizontal winds over a range of wave-length from about five diameters to the earth's circumference. Note the  $k^{-3}$  and  $k^{-5/3}$  slopes (after Lilly 1983).



**Fig. 1.7** The boundary layer in high pressure regions over land consists of three major parts: a very turbulent mixed layer; a less-turbulent residual layer containing former mixed-layer air; and a nocturnal stable boundary layer of sporadic turbulence. The mixed layer can be subdivided into a cloud layer and a subcloud layer. Time markers indicated by S1-S6 will be used in Fig. 1.12.

### Direct Numerical Simulation (DNS)

This method implies a full un-truncated numerical solution of the Navier-Stokes equations without any "closure-technique" or parameterisation implied.

While DNS-methods has proven successful to low-Reynolds number application and study cases within the field of computational fluid dynamic (eg. in the study of vortex-interaction in a low-Reynolds number two-dimensional fluid), application of DNS to fully developed boundary layer turbulence is out of the question because of the multitude of scales involved. In order to model atmospheric turbulence and diffusion in just one cubic Km using DNS, approximately  $10^{18}$  grid points would be required. This is because the smallest length scale in atmospheric turbulence (the Kolmogorov's length scale) is of the order of 1 mm only so that each of the 3 spatial dimensions require about  $10^6$  grid points. In addition must be considered the corresponding integration time requirements. DMS techniques are therefore beyond any conceivable modelling capability based on known computer platforms for modelling of the detailed flow and diffusion patterns in the atmosphere.

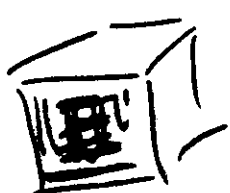
Parameterisation of turbulence and diffusion processes in the atmosphere will consequently always be required.

## Direct Numerical Simulation (DNS)

This method implies a full un-truncated numerical solution of the Navier-Stokes equations without any "closure-technique" or parameterisation implied.

While DNS-methods has proven successful to low-Reynolds number separated flow around bodies within the field of computational fluid dynamic (eg. in the simulation of the interaction in a low-Reynolds number two-dimensional field), application of DNS to fully developed boundary layer turbulence is out of the question because of the large range of scales involved. In order to model atmospheric turbulence and diffusion in a realistic manner using DNS, approximately  $10^{10}$  grid points would be required to resolve the smallest length scale in atmospheric turbulence (the Kolmogorov's length scale) which is of the order of 1 mm only so that each of the 3 spatial dimensions requires about 10<sup>3</sup> grid points. In addition must be considered the corresponding integration time requirements. DNS techniques are therefore beyond any conceivable modelling capability based on known computer platforms for modelling of the detailed flow and diffusion patterns in the atmosphere.

Parameterisation of turbulence and diffusion processes in the atmosphere will consequently always be required.



$$1 \text{ km}^3 \Rightarrow 10^8 \text{ grid points } \tilde{n}.$$

Simpler approach: Diffusion theory.

ex. 1

Mean-Transport:

$$C = \bar{C} + C'$$

$$\frac{d\bar{C}}{dt} = -\nabla \cdot \text{flux} ; \text{ flux} = -\nabla \bar{C} \cdot K$$

K?

- 1) *Statistical theory*,  
including single and multiple particle  
releases and Monte Carlo-techniques
- 2) *Similarity theory*,
- and
- 3) *Gradient transport (K-theories)*

## Statistical Theory (G.I. Taylor's formula)

Taylor established, in his pioneering work from 1921, a relationship between the plume width (standard deviation  $\sigma$ ) and the Lagrangian auto-correlation of the dispersing fluid, which in this case is the turbulent atmosphere.

Define:

$\sigma_y^2(t)$  Mean square crosswind deviation from fixed axis at time  $t$ .

$v(t)$  Crosswind fluid or particle velocity in a homogeneous field of turbulence.

$R_L(\tau)$  The corresponding Lagrangian (single-particle) autocorrelation function  $\langle v(t)v(t+\tau) \rangle$ .

### • Absolute (fixed frame) single-particle diffusion: Plumes

G.I. Taylor related the growth rate of the average plume width  $\sigma$ , to the Lagrangian autocorrelation of the atmospheric turbulence. The formula applies to the ensemble-averaged plume width including plume meander, in a coordinate system fixed to the source point.

To distinguish Taylor diffusion from the turbulent diffusion of an instantaneously released multiple-particle puff, in which case the coordinate system moves with the puff's center of mass (see below), Taylor diffusion is often referred to as *absolute* or *fixed frame* or *single-particle* diffusion.

*Taylor's formula* for plume diffusion reads:

$$\frac{1}{2} \frac{d\sigma_y^2}{dt} = \int_0^t R_L(\tau) d\tau = \overline{v^2} t_e(t) \quad (6.1)$$

where  $\langle v^2 \rangle$  denotes the variance or the velocity (square) scale of the turbulence, and  $t_e$  denotes the corresponding *time scale* or *memory time* for the *diffusion process*.

## PLUMES, cont.:

### Asymptotic limits:

In the limit for large *travel times* or *diffusion times*,  $t_s(\infty)$  defines the Lagrangian *integral time scale*  $t_L$  through:

$$\int_0^\infty R_L(\tau) d\tau = \overline{v^2} t_L \quad (6.2)$$

Taylor's formula, Eq. (6.1), yields in this limit the corresponding *far field* solution:

$$\sigma_y^2 = 2 \overline{v^2} t_L t \quad (6.3)$$

In the opposite limit, with *travel times* or *diffusion times* much smaller than the Lagrangian integral time scale:  $t < t_L$ , the auto-correlation function becomes:  $R_L(\tau) \sim 1$  and Taylors formula results in the so-called *near-field* solution:

$$\sigma_y^2 = \overline{v^2} t^2 \quad (6.4)$$

### Spectral form:

By introduction of the Lagrangian *variance spectrum*  $S_L(\omega)$ :

$$\overline{v^2} S_L(\omega) = \frac{1}{2\pi} \int_{-\infty}^{\infty} R_L(\tau) e^{-i\omega\tau} d\tau \quad (6.5)$$

Taylor's formula can be represented in its corresponding spectral form:

$$\frac{1}{2} \frac{d\sigma_y^2}{dt} = \overline{v^2} t^2 \int_{-\infty}^{\infty} S_L(\omega) \frac{\sin^2(\omega\tau/2)}{(\omega\tau/2)^2} d\tau \quad (6.6)$$

- PUFFS

### Relative (moving frame) multiple-particle diffusion: Puffs

An analogous Taylor's formula for puff diffusion, relating the ensemble averaged puff standard deviation  $\sigma_p$  to some turbulence property of the flow, can be formulated in terms of *relative* fluid particle velocities  $v_r(t)$ .

Define:

$\sigma_p^2(t)$ : Mean square crosswind deviation about puff's center-of-mass.

$v_r(t)$ : Crosswind particle velocity relative to puff's center-of-mass velocity.

$R_r(t, \tau)$ : Lagrangian auto-correlation function for  $v_r$ :  $\langle v_r(t)v_r(t+\tau) \rangle$ .

In these terms, Taylor's formula for relative diffusion then reads:

$$\frac{1}{2} \frac{d\sigma_p^2}{dt} = \int_0^t R_r(t, \tau) d\tau = \overline{v_r^2} t_r(t) \quad (6.7)$$

\* This equation applies to the ensemble-averaged instantaneous puff size relative to the puff's center-of-mass coordinate. To distinguish the spread in Eq (7) from the diffusion of a plume (Eq. (1)), puff diffusion is often referred to as *relative*, *moving frame* or *two-particle* diffusion.

*Moving frame diffusion*, ( $\sigma_p^2$ ), plus *center-of-mass meandering*, ( $X_{cm}^2$ ), equals *fixed frame diffusion* ( $\sigma_s^2$ ).

The relative velocity and time scales defined by Eq. (7) can for Gaussian shaped puffs be modelled as (Mikkelsen et al., 1986):

$$\overline{v_r^2} = \overline{v^2} \int_{-\infty}^{\infty} S_E(k) (1 - e^{-k^2 \sigma_L^2}) dk \quad (6.8)$$

$$t_r(t) = \frac{1}{\overline{v_r^2}} \int_0^t R_L(\tau) d\tau \quad (6.9)$$

where  $S_E(k)$  is the fixed point Eulerian covariance spectrum and  $R_L(\tau)$  the single-particle Lagrangian auto-correlation function. quantities.

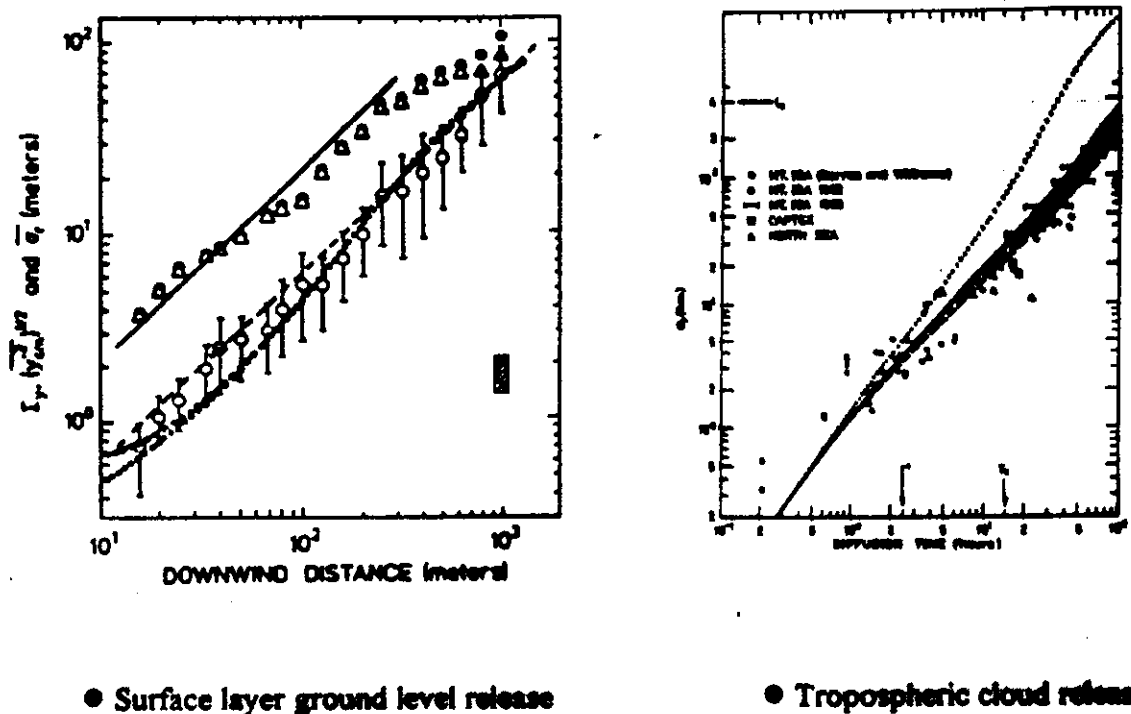


Figure 6.1 Relative and absolute diffusion on different scales. The left figure shows diffusion of ground level released smoke to distances out to 1 km from the source. The lower set of data points shows the observed puff diffusion whereas the upper set of points and represents plume diffusion including meander. The solid lines show model results based on Eqs (7)-(9) (lower) and on Eq.(1) (upper), and represents puff and plume diffusion respectively. The right Figure shows tropospheric puff diffusion data observed on the meso- $\alpha$  scale. Plume diffusion has here no meaning on this scale and consequently is only cloud or puff diffusion shown. The model results (lines) are calculated by the puff model in Eq.(7)-(9). (Mikkelsen & Eckman, 1983), (Mikkelsen et. al., 1988).

$h \approx 8 \text{ km}$  (IR temperature)

ex#11.

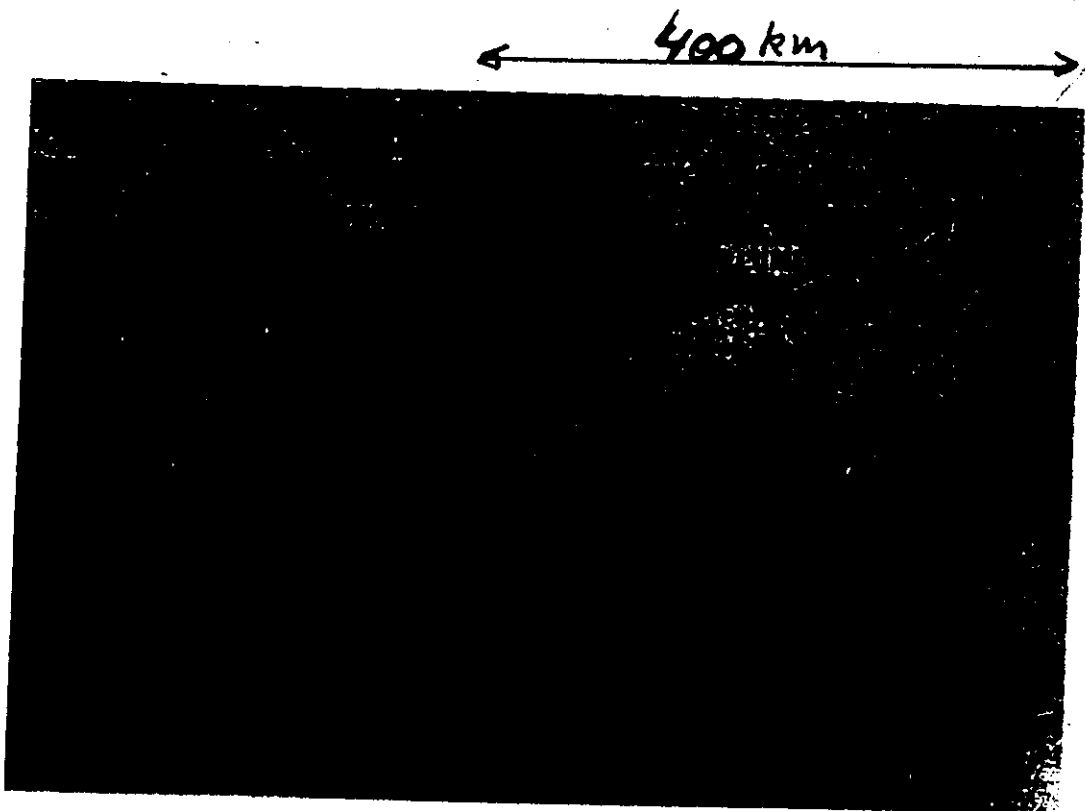


Figure 1. TIRAO thermal IR image of Novaya Zemlya plume on Feb. 11, 1986 (Platson, 1986).

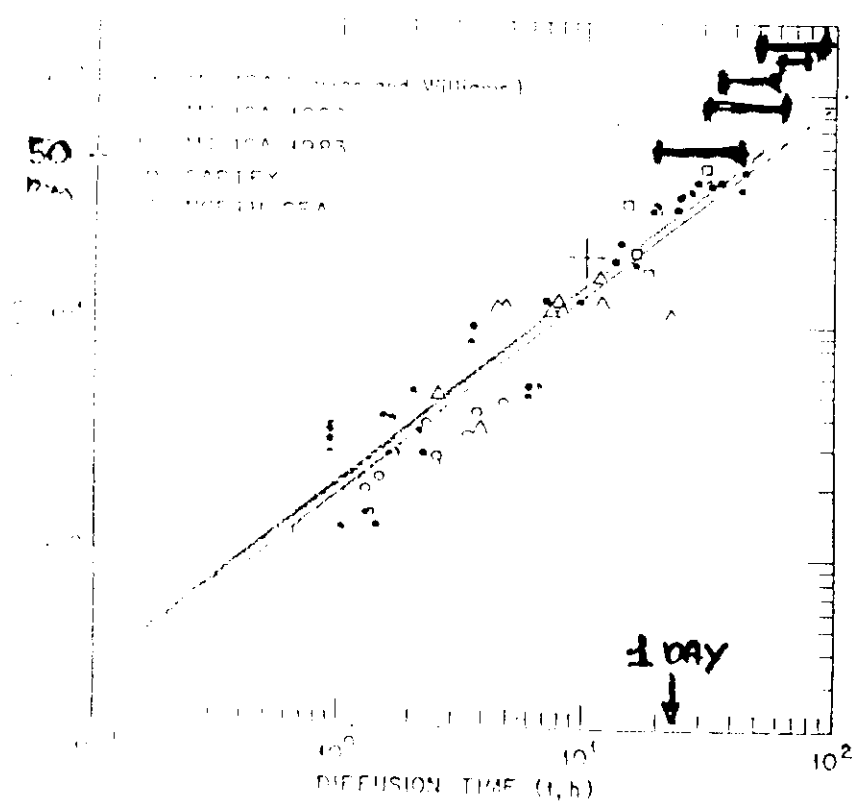


Figure 2. Cloud width,  $\sigma_y$ , as a function of diffusion time, for previous data,<sup>y</sup> (Gifford, 1985), showing the Novaya Zemlya plume (large cross).

## Statistical Theory (Monte-Carlo Techniques)

### • Homogeneous turbulence

- $v(t)$ : Crosswind turbulent particle velocity
- $1/\beta$ : Lagrangian memory time scale  $t_L$
- $\rho_L(\Delta t)$ : Lagrangian auto-correlation  $e^{-T}$ ,  $T = \Delta t/t_L$
- $a(t)$ : Random uncorrelated accelerations  $\langle a(t_1)a(t_2) \rangle$

Random force model - Langevin equation:

$$\frac{dv}{dt} + \beta v = a(t) \quad (6.10)$$

Corresponding Markov equation:

$$v(t+\Delta t) = \rho_L(\Delta t)v(t) + \eta(t) \quad (6.11)$$

where  $\eta(t)$  is a Gaussian process ( $\mu=0$ ;  $\sigma_\eta^2 = (1-\rho^2)\langle v^2 \rangle$ ).

### Solutions:

Fixed frame - absolute diffusion (Taylor's formula):

$$\sigma_v^2 = 2\bar{v}^2 t_L^2 [T - (1 - e^{-T})] \quad (6.12)$$

Moving frame - "relative diffusion" ( $v_r(0)=0$  (Gifford, 1982)):

$$\sigma_{v_r}^2 = 2\bar{v}^2 t_L^2 [T - (1 - e^{-T}) - (1 - e^{-T})^2] \quad (6.13)$$

i.e.:

Moving frame diff = Fixed frame diff - meander

• Inhomogeneous Gaussian turbulence

$P(w)$ : Vertical ( $w$ ) velocity pdf (Gaussian)

$\sigma_w, t_L$ : functions of vertical coordinate  $z$

Corresponding in-homogeneous Markov equation (Wilson et al., (1983); Legg and Rempach (1982)):

$$w(t+\Delta t) = aw(t) + b\sigma_w \eta(t) + (1-a)t_L d\sigma_w^2/dz \quad (6.14)$$

where  $a = \exp(-\Delta/t_L)$  and  $b = (1-a^2)^{1/2}$ .

• Inhomogeneous non-Gaussian turbulence (well mixed)

Thomson (1987), Luhar and Britter (1989), Tassone (1993)

$P(z,w)$ : Joint (non-gaussian) pdf of  $(z,w)$ .

Fokker-Planck eqs:

$$w \frac{\partial P}{\partial z} + \frac{\partial}{\partial w}(aP) = \frac{1}{2} \frac{\partial^2}{\partial w^2}(b^2 P) \quad (6.15)$$

The corresponding Markov equations are obtained from:

- 1) Specify  $P'(w)$  and  $P(w)$  (skewed up/down-draft pdf).
- 2) Assume local isotropy (Kolmogorov subrange:  $b = (c_* e)^{1/2}$ ).
- 3) Solve Fokker-Planck for  $a$ , then integrate the corresponding non-linear stochastic Markov DE<sup>n</sup>:

$$dw = a(z,w)dt + b(z,w)d\eta \quad (6.16)$$

$$dz = wdt$$



Figure 6.2 Deardon/Willis water tank (Hanna, 1982)

# Langevin models for inhomogeneous and skewed turbulence

Thomson (1987) Method

Known skewed and/or inhomogeneous  
 $P_q(w, z)$  of ambient air

**Well-mixed condition:**  
 $P(w, z, t \rightarrow \infty) \approx P_a(w, z)$

Kolmogorov theory of local isotropy +  
Gaussian random forcing

$$\rightarrow b^2 = C_0 \varepsilon$$

Fokker-Planck equation:

$$\frac{\partial P}{\partial t} = -\frac{\partial}{\partial z}(wP) + \frac{\partial}{\partial w}\left(-aP + \frac{1}{2}b^2 \frac{\partial P}{\partial w}\right)$$

With  $P$  and  $b$  known, solve for  $a$

$$a, b$$

Langevin equation:

$$dw = -adi + bd\zeta$$

## Two-Particle Statistics, Distance Neighbour-function and Concentration Fluctuations:

### • Concentration Mean $\langle c \rangle$ and Variance $\langle c^2 \rangle$ :

Define:

$\langle c \rangle$ : Mean concentration

$\langle c(y_1, t)c(y_2, t) \rangle$ : Concentration co-variance

$S(y)$ : Source distribution at time  $t_0$

$P_1(y, t; y', t_0)$ : One-particle transition probability in time interval  $t-t_0$ .

$P_2(y_1, y_2, t; y'_1, y'_2, t_0)$ : Joint two-particle transition probability in time interval  $t-t_0$ .

Then, accordingly to Batchelor (1952), Durbin (1984):

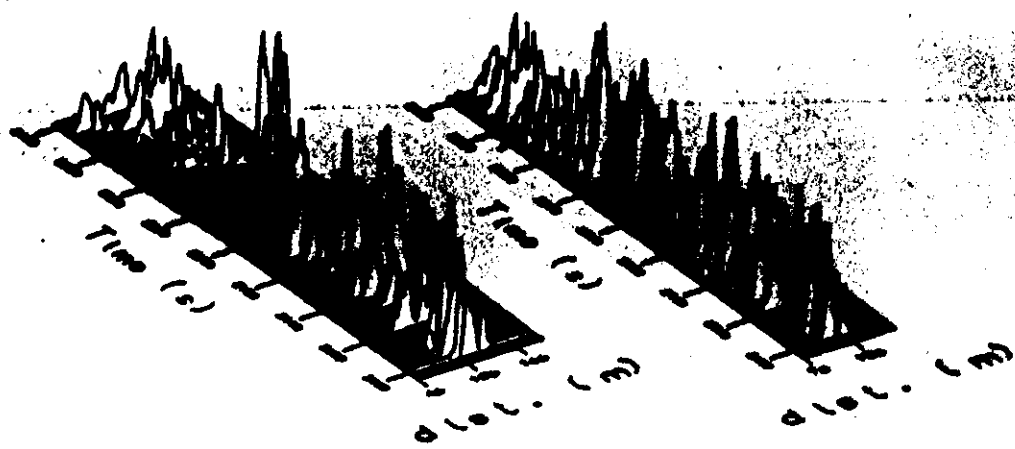
$$\bar{c}(y, t) = \int P_1(y, t; y', t_0) S(y') dy' \quad (6.18)$$

$$\bar{c^2}(y, t) = \iint P_2(y, y, t; y_1, y_2, t_0) S(y_1) S(y_2) dy_1 dy_2 \quad (6.19)$$

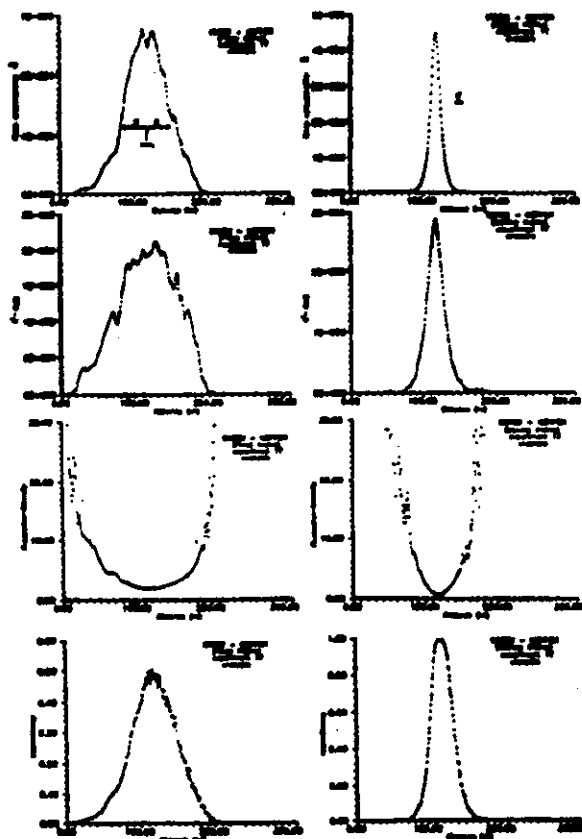
Note:  $\langle c^2 \rangle$  and thereby concentration fluctuations ( $c'$ ),  
 $(\langle c'^2 \rangle = \langle c^2 \rangle - \langle c \rangle^2)$ , relates to two-particle statistics!

## Lidar Measurements of Plume Statistics :

- Crosswind concentration profiles (Jørgensen & Mikkelsen, 1993):



- Figure 6.3 Lidar measurements: Fixed frame (left) and moving frame (right)



- Figure 6.4: Crosswind plume statistics of  $\langle c \rangle$ ,  $\langle c^2 \rangle$ , Intensity and Intermittency: Left side: Fixed frame; Right side: Moving Frame.

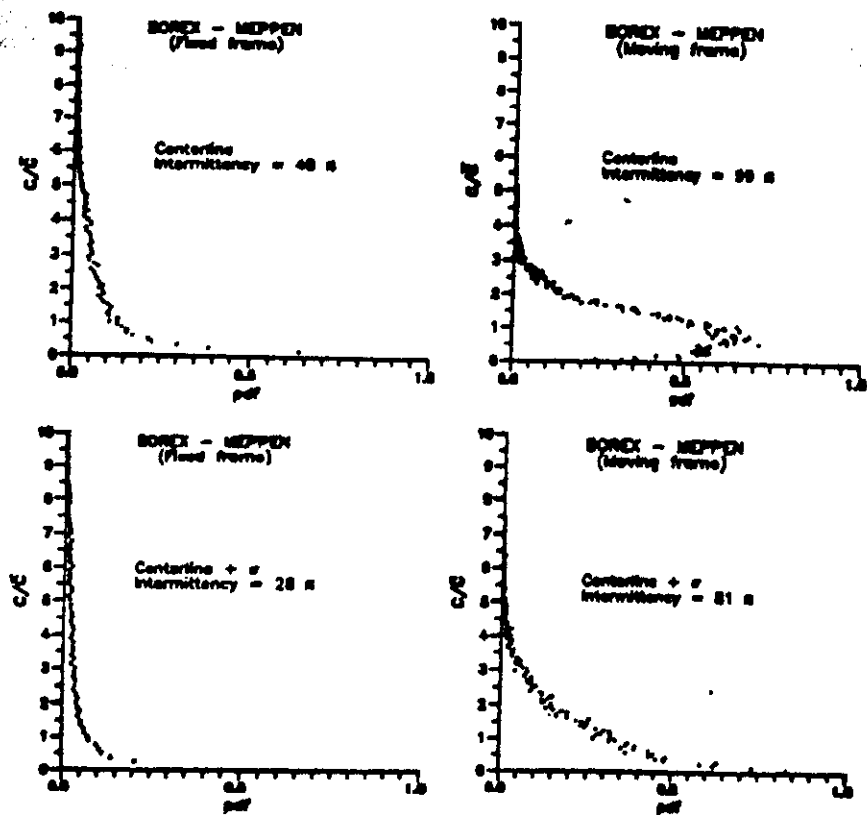


**Figure 6.5: Measured concentration pdf's.**  
**Left side: Fixed Frame. Right side: Moving frame**  
**Top: Centerline. Bottom: Plume margin ( $\pm 1\sigma$ ).**

## Distance-neighbour Functions:

Define: Distance Neighbour function (Richardson, 1926):

$$q(l) = \int_{-\infty}^{\infty} c(y) c(y+l) dy \quad (6.20)$$

Diffusion eq. for  $q(l)$ :

$$\frac{\partial}{\partial t} q(l,t) = \frac{\partial}{\partial l} K(l) \frac{\partial}{\partial l} q(l,t) \quad (6.21)$$

Richardson, 1926:  $K(l) \propto l^{4/3}$ ; (note:  $\sigma_p^2 \propto eT^3$ ),  
 Batchelor, 1952:  $K(l) \propto \langle l^2 \rangle^{2/3}$ ; (note:  $\langle l^2 \rangle = 2\sigma_p^2$ ).

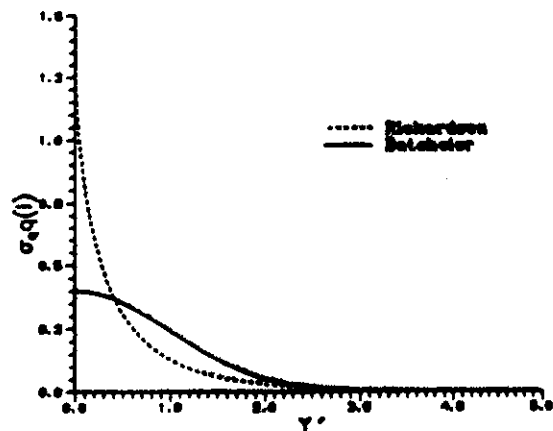
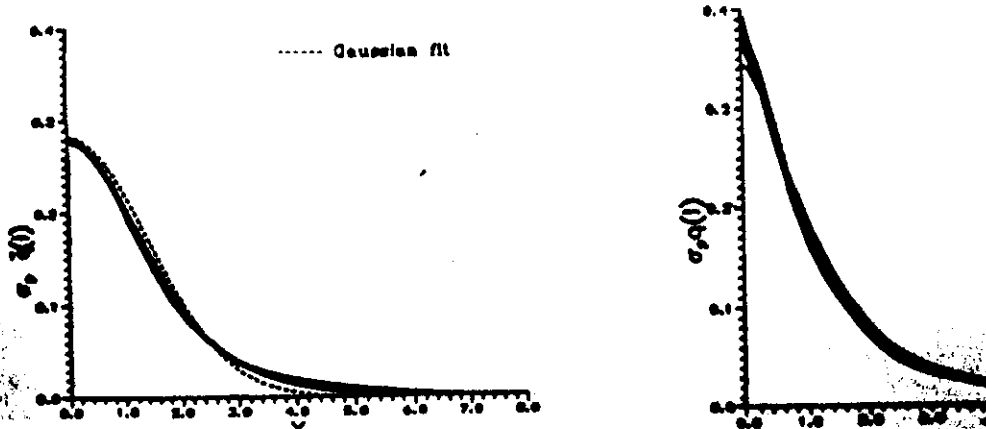


Figure 6.6  
Solutions to  $q(l)$  diffusion eq.



• Resent Lidar measurements (Jorgensen and Mikkelsen, 1993):

### Lagrangian Similarity Theory (Batchelor 1964):

- Continuous line source, ground level release.

Define:  $\langle Z \rangle$ : Mean vertical plume height

$$\frac{d\bar{Z}}{dt} = cu_* g\left(\frac{z}{L}\right) \quad (6.22)$$

- Instantaneous Source: Relative diffusion (Batchelor, 1950):

$$\frac{1}{2} \frac{d\sigma_p^2}{dt} \propto t(\epsilon\sigma_o)^{2/3}; \text{ small } t \text{ limit} \quad (6.23)$$

$$\frac{1}{2} \frac{d\sigma_p^2}{dt} \propto \epsilon t^2; \text{ intermediate } t \quad (6.24)$$

$$\frac{1}{2} \frac{d\sigma_p^2}{dt} \propto \overline{v^2} t_L; \text{ large } t \quad (6.25)$$

## Gradient Transport - K Theories :

### 1. The Diffusion Equation

- Conservation principle

$$\frac{dc}{dt} = \frac{\partial c}{\partial t} + u_i \frac{\partial c}{\partial x_i} = 0 \quad (6.26)$$

Reynolds decomposition (e.g.  $c = \langle c \rangle + c'$ ;  $\langle c' \rangle = 0$ ) leads to the:

- Diffusion equation:

$$\frac{\partial \bar{c}}{\partial t} + u_i \frac{\partial \bar{c}}{\partial x_i} = - \frac{\partial}{\partial x_i} \bar{u}_i c' + \text{sources} - \text{sinks} \quad (6.27)$$

### 2. Gradient Transport: K - closure:

In analogy to "exact" molecular diffusion:

- First order closure

$$\bar{u}_i c' = - K_i \frac{\partial \bar{c}}{\partial x_i} \quad (6.28)$$

+ : Eulerian  
easy applicable

- : No memory,  $t \gg t_0$

### 3. Analytical Solution of the Diffusion Equation:

Assume one-dimension ( $y$ );  $K_z$  and  $\langle u \rangle$  are constants  $\neq 0$ :

$$\frac{\partial \bar{c}}{\partial t} = - \frac{\partial \bar{c}}{\partial z} = \frac{\partial}{\partial z} (K_z \frac{\partial \bar{c}}{\partial z}) = K_z \frac{\partial^2 \bar{c}}{\partial z^2} \quad (6.29)$$

- Solution:

$$\bar{c}(z, t) = \frac{Q}{\sqrt{2\pi} u \sigma_z} e^{-\frac{1}{2} \left(\frac{z}{\sigma_z}\right)^2} \quad (6.30)$$

where  $\sigma_z^2(t) = 2K_z t + \sigma_z^2(0)$ , since  $\frac{1}{2} d\sigma_z^2/dt = K_z$ .  
Analytical solutions also exists when  $\langle u \rangle$  and  $K_z$  are power functions in  $z$ .

#### $\sigma_y$ , $\sigma_z$ , and $\sigma_r$ Classification Schemes:

2-D solution to the diffusion equation, constant coefficients, is

$$\bar{c}(y, z) = \frac{Q}{2\pi u \sigma_y \sigma_z} e^{-\frac{1}{2}(\frac{y}{\sigma_y})^2 - \frac{1}{2}(\frac{z}{\sigma_z})^2} \quad (6.31)$$

where  $\sigma_y$  and  $\sigma_z$  are given as functions of the Pasquill-Gifford Turner (PGT) stability schemes, viz.:

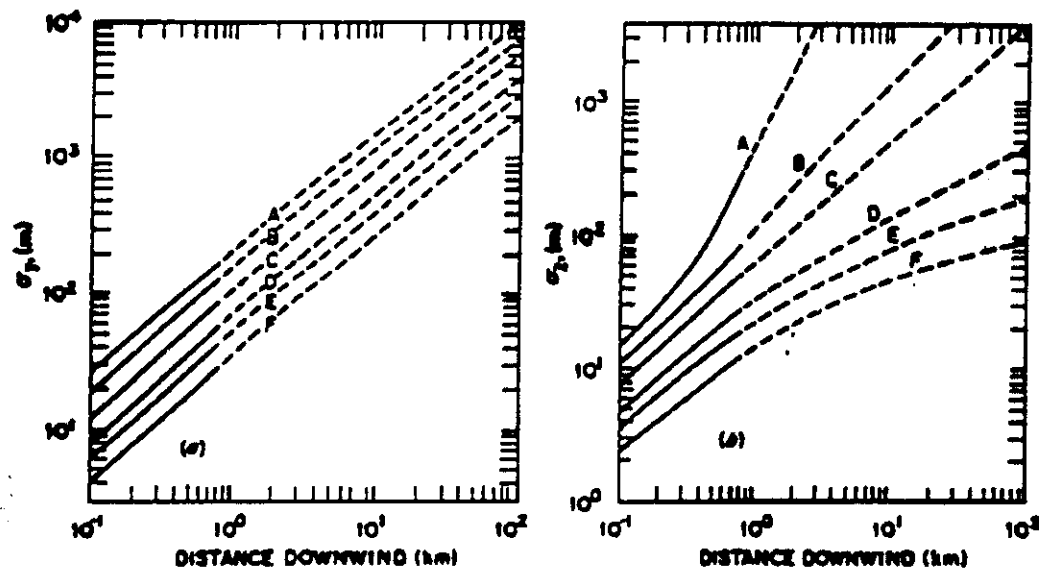


Figure 6.8

5. Next Generation of Practical Short-range Dispersion Models  
 (ref. Olesen and Mikkelsen, 1992):

- Formula-based, similarity scaling ( $u_*$ ,  $L$ ,  $z_*$ ,  $w_*$ ):

$$\sigma_y = \sigma_0 \bar{u} t F_y(u_*, w_*, L, z_*, z) \quad (6.32)$$

$$\sigma_z = \sigma_0 \bar{w} t F_z(u_*, w_*, L, z_*, z) \quad (6.33)$$

- Examples from the Danish OML model:

Unstable atmosphere, elevated release:

$$\sigma_z^2 = 0.33 w_*^2 t^2 + 1.2 u_* t^2$$

Stable atmosphere,  $z > L$ :

$$T_L = 0.45 L/u_*$$

*"From:  
the book!"*

6. Similarity theory for  $K_s$ :

- Surface layer (Businger et.al., 1971):

$$K_s = \frac{\kappa u_* z}{\Phi_h(z/L)} \quad (6.34)$$

where  $\kappa$ : von Kármán's constant, and  $\Phi_h$ : Dimensionless temperature gradient (for heat).

- Boundary Layer (Hanna, 1968)

$$K_s = 0.15 \sigma_w \lambda_m \quad (6.35)$$

where

$\sigma_w$ : Vertical variance.

$\lambda_m$ : Peak wavenumber in  $w$ -spectrum (Kaimal et al. 1976).

## 7. Spectral Closure of the Diffusion Eqs.:

Fourier-transforming the diffusion eqs (1-D in z) leads to (Troen et. al., 1980):

$$\frac{d}{dt} \tilde{c}(k,t) = -k^2 K(k) \tilde{c}(k,t) \quad (6.36)$$

where  $\frac{1}{2} d\sigma_z^2/dt = K_z(\sigma(t)) = K_z(\alpha/k)$ ; [non-local gradient].

## 4 Diffusion Parameterization in Meso-scale Models

### 1 A Linearized Model for Terrain-induced Flow ( Santabarbara et al. 1993)

$$\begin{aligned} U_0 \frac{\partial u}{\partial x} + V_0 \frac{\partial u}{\partial y} &= -\frac{\partial p}{\partial x} + fv + K \frac{\partial^2 u}{\partial z^2}, \quad \frac{\partial u}{\partial z} + \frac{\partial v}{\partial y} + \frac{\partial w}{\partial z} = 0, \\ U_0 \frac{\partial v}{\partial x} + V_0 \frac{\partial v}{\partial y} &= -\frac{\partial p}{\partial y} - fu + K \frac{\partial^2 v}{\partial z^2}, \quad U = U_0(c_1 |\alpha|^{-1}), \\ U_0 \frac{\partial w}{\partial x} + V_0 \frac{\partial w}{\partial y} &= -\frac{\partial p}{\partial z} + K \frac{\partial^2 w}{\partial z^2} + \frac{g}{\pi} \tilde{Q}, \quad K = K(c_2 |\alpha|^{-1}), \end{aligned}$$

Figure 6.9

Restrictions:

- Near-neutral stratification.
- Surface-layer profiles for  $\langle u \rangle$  and  $K_r$ .

Boundary Conditions:

- $\langle u \rangle \nabla h(x, y) = w(0)$ ;  $h(x, y)$  is terrain.

Closure:

- Spectral  $K(k) = K(\alpha/k)$

Solution:

- Analytic in  $z$  for each wave-number, viz.:

$$u(k, z) = k \bar{f}(k) \bar{u}(k) (e^{-kz} - e^{-\frac{k+im\sqrt{2}}{L}}) \quad (6.37)$$

where:

- $\bar{h}(k)$ : Fourier-transformed terrain,  
 $L = 1/k$ : Outer length scale (inviscid limit),  
 $l(k)$ : Inner length scale, below which stress-influences.

Summary:

- + : Modest computational effort
- : Truncated physics, 1. order perturbations only

## Neutral flow

$$\vec{u}_o(z) = (u_o(z), v_o(z)) = \frac{u_{*o}}{\kappa} \ln\left(\frac{z}{z_o}\right) \vec{n}_o$$

$$K(z) = u_{*o} \kappa z$$

Flow model LINCOM (Troen and de Baas, 1986)

$$U_o = U_o(c_1|\alpha|^{-1})$$

$$K = K(c_2|\alpha|^{-1})$$

$$\alpha_1 = \frac{\sqrt{2}}{2}(i-1)\ell^{-1} \text{ with } \ln\left(\frac{c_1\ell}{z_o}\right) = c_2\kappa^2 L$$

and

$$\alpha_2 = -|\kappa| = -L^{-1}$$

Line AA

Height 10m Upwind direction 210 degrees

2.0

Norm. Speed

1.5

1.0

0.5

0.0

-0.5

CP

0.0 0.5 1.0

Distance from CP (1000m)

AA

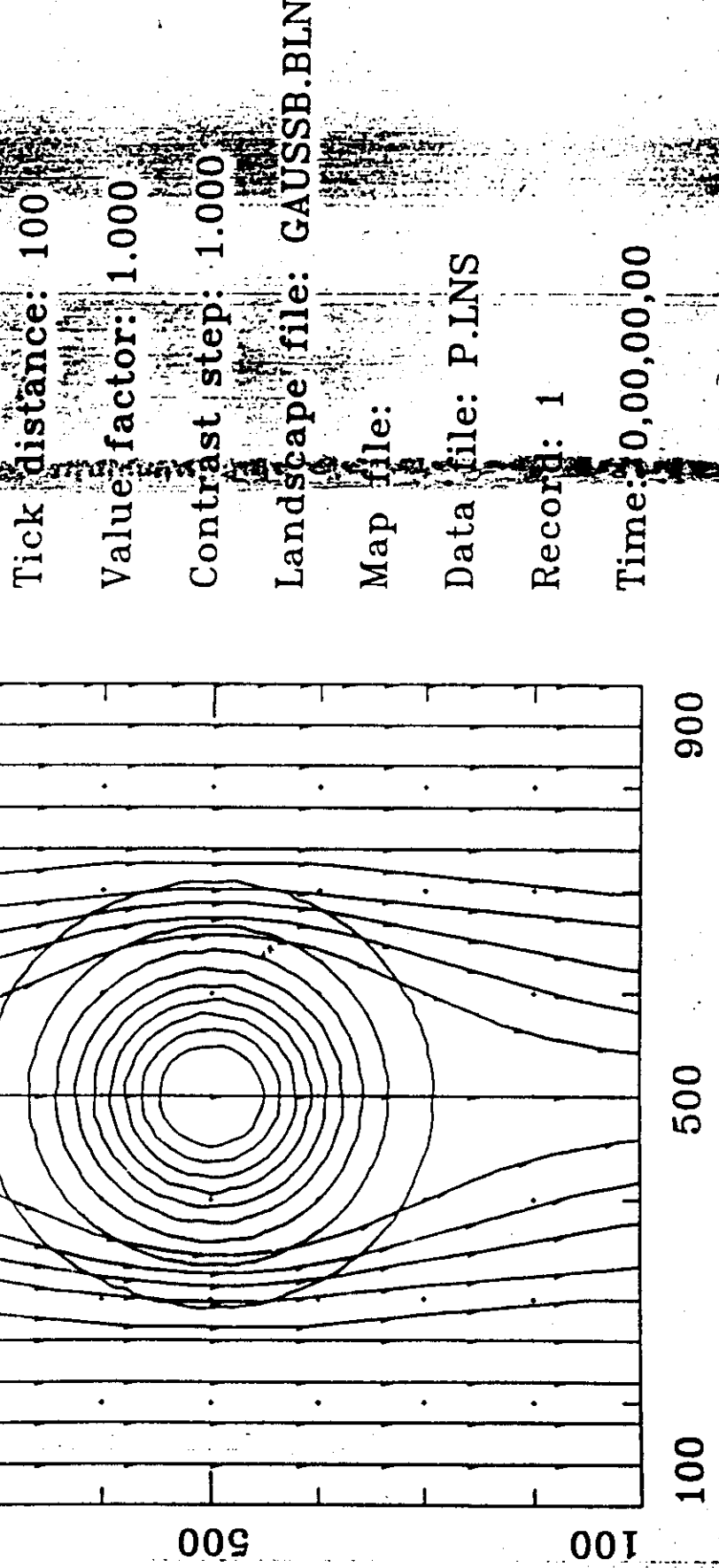
shear

Thermal

$\kappa \neq 0$   $g^l > 0$

S, Oct 92

Plot: 20/5/1994



unstable

Thermal

to g < 0

S, Oct'92

Plot: 20/5/1994

Tick distance: 100

Value factor: 1.000

Contrast step: 1.000

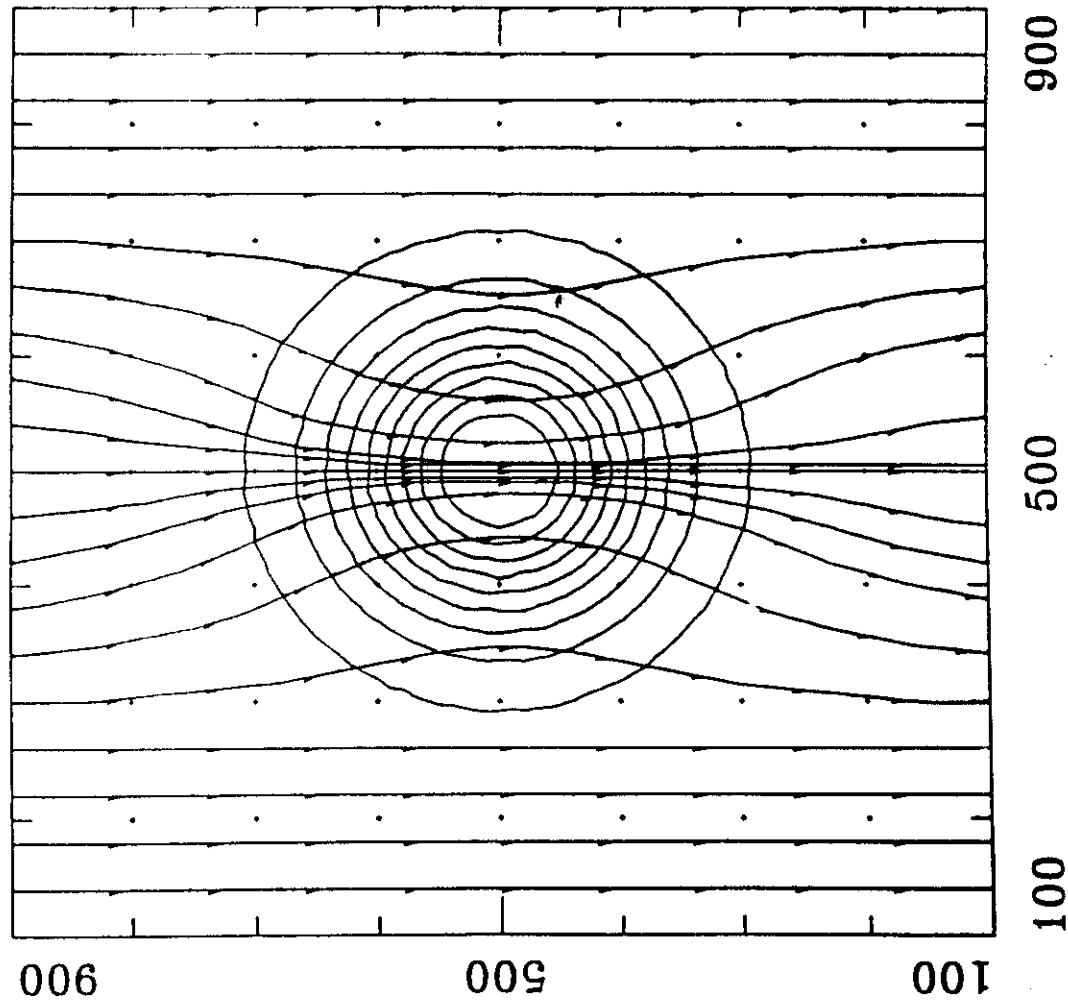
Landscape file: GAUSSB.BLN

Map file:

Data file: N.LNS

Record: 1

Time: 0,00,00,00



## 2 Mesoscale - Primitive Equation based Diffusion:

Assume:

- Navier Stokes Eqs.
- Boussinesq approximation ( $\rho$  only in  $w$ :  $\delta\rho/\rho = g'$ ).
- Shallow system ( $\partial u_j/\partial x_j = 0$ )
- Small slopes
- Hydrostatic assumption

Corresponding conservation equations in terrain following coordinates (Pielke, 1984):

$$\frac{\partial}{\partial \tilde{x}^j} \rho_0 \frac{s - z_G}{s} \tilde{u}^j = 0,$$

$$\frac{\partial \tilde{u}^1}{\partial t} = -\tilde{u}^j \frac{\partial \tilde{u}^1}{\partial \tilde{x}^j} + \left( \frac{s}{s - z_G} \right)^2 \frac{\partial}{\partial \tilde{x}^3} K_M \frac{\partial \tilde{u}^1}{\partial \tilde{x}^3} - \overline{\tilde{u}^{j''} \frac{\partial \tilde{u}^{1''}}{\partial \tilde{x}^j}} \Big|_{j=1,2} \\ - \bar{\theta} \frac{\partial \bar{\pi}}{\partial \tilde{x}^1} + g \frac{\sigma - s}{s} \frac{\partial z_G}{\partial x} - \tilde{f} \tilde{u}^3 + \tilde{f} \tilde{u}^2,$$

$$\frac{\partial \tilde{u}^2}{\partial t} = -\tilde{u}^j \frac{\partial \tilde{u}^2}{\partial \tilde{x}^j} + \left( \frac{s}{s - z_G} \right)^2 \frac{\partial}{\partial \tilde{x}^3} K_M \frac{\partial \tilde{u}^2}{\partial \tilde{x}^3} - \overline{\tilde{u}^{j''} \frac{\partial \tilde{u}^{2''}}{\partial \tilde{x}^j}} \Big|_{j=1,2} \\ - \bar{\theta} \frac{\partial \bar{\pi}}{\partial \tilde{x}^2} + g \frac{\sigma - s}{s} \frac{\partial z_G}{\partial y} - \tilde{f} \tilde{u}^1,$$

$$\frac{\partial \bar{\pi}}{\partial \tilde{x}^3} = -\frac{g}{\bar{\theta}} \frac{s - z_G}{s},$$

$$\frac{\partial \bar{\theta}}{\partial t} = -\tilde{u}^j \frac{\partial \bar{\theta}}{\partial \tilde{x}^j} + \left( \frac{s}{s - z_G} \right)^2 \frac{\partial}{\partial \tilde{x}^3} K_\theta \frac{\partial \bar{\theta}}{\partial \tilde{x}^3} - \overline{\tilde{u}^{j''} \frac{\partial \theta''}{\partial \tilde{x}^j}} \Big|_{j=1,2} + \tilde{S}_\theta,$$

$$\frac{\partial \bar{q}_n}{\partial t} = -\tilde{u}^j \frac{\partial \bar{q}_n}{\partial \tilde{x}^j} + \left( \frac{s}{s - z_G} \right)^2 \frac{\partial}{\partial \tilde{x}^3} K_\theta \frac{\partial \bar{q}_n}{\partial \tilde{x}^3} - \overline{\tilde{u}^{j''} \frac{\partial q_n''}{\partial \tilde{x}^j}} \Big|_{j=1,2} + \tilde{S}_{q_n},$$

$$\frac{\partial \bar{\chi}_m}{\partial t} = -\tilde{u}^j \frac{\partial \bar{\chi}_m}{\partial \tilde{x}^j} + \left( \frac{s}{s - z_G} \right)^2 \frac{\partial}{\partial \tilde{x}^3} K_\theta \frac{\partial \bar{\chi}_m}{\partial \tilde{x}^3} - \overline{\tilde{u}^{j''} \frac{\partial \chi_m''}{\partial \tilde{x}^j}} \Big|_{j=1,2} + \tilde{S}_{\chi_m},$$

Figure 6.10 RAMS

### 3 Prandtl type Closure:

- Prandtl (1932):

$$K \approx l^2 \left| \frac{du}{dz} \right| \quad (6.38)$$

Example: Let  $d\langle u \rangle / dz = Ku/z \rightarrow K = Ku.z$

Problems occur at  $d\langle u \rangle / dz \approx 0$  (no flux).

### 4 One-eqs. models:

- Prandtl & Kolmogorov (1940's)

$$K \approx c_k l \sqrt{\epsilon^2} \quad (6.39)$$

where

$\epsilon^2$ : Turbulent Kinetic Energy (TKE equation required).  
l: length scale (local flow), eg.

- Blackadar (1962):

$$l = \frac{K(z-z_o)}{1 + \frac{K(z-z_o)}{l_*}} \quad (6.40)$$

with  $l_* = 10 - 25$  meters.

## 5 Two-eqs. K- $\epsilon$ models:

In a K- $\epsilon$  model are "memory effects" introduced in the diffusivity parameter K in order to reflects the upstream history of the flow. This is accomplished by introduction of an additional transport equation for the dissipation quantity itself  $\epsilon$  (or alternatively through an equation for its related length scale parameter  $l_\epsilon$ , see Launder and Spalding (1974)).

### Two-equation K- $\epsilon$ model:

Harlow & Nakayama (1968) proposed that the turbulent diffusivity could be expressed in terms of:

1) The Total Kinetic Energy:  $e^2$  [ $m^2/s^2$ ], and

2) The TKE's dissipation rate  $\epsilon$ : [ $m^2/s^3$ ], - or its corresponding length scale  $l_\epsilon$ , as:

$$K = c_\mu \frac{(e^2)^2}{\epsilon} = \frac{c_1}{c} e l_\epsilon \quad (6.41)$$

where

$$\epsilon = c \frac{e^3}{l_\epsilon} \quad (6.42)$$

The turbulent kinetic energy is in a K- $\epsilon$  model obtained from the TKE-equation in the usual form:

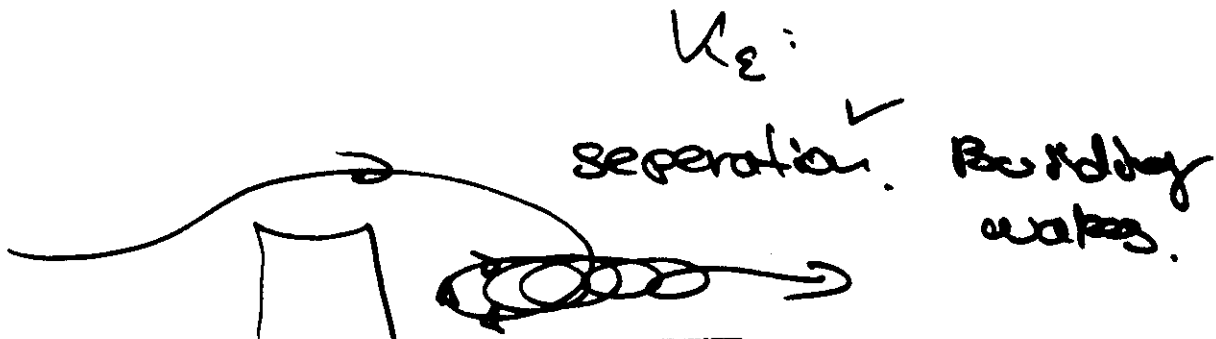
$$\frac{de^2}{dt} = \text{production} + \text{diffusion} - \frac{\epsilon^3}{l_\epsilon} \quad (\text{TKE}) \quad (6.43)$$

whereas a second transport equation for  $\epsilon$  is added:

$$\frac{d\epsilon}{dt} = \text{production} + \text{diffusion} - \frac{\epsilon^2}{e^2} \quad (\text{Dissipation eqs.}) \quad (6.44)$$

### Solution:

Eqs. 43 and 44 are solved simultaneously for  $e$  and  $\epsilon$ . The diffusivity K is then given directly as:  $c_\mu e^4/\epsilon$ , or alternatively, by use of Eq. 42, in terms of a turbulent velocity and length scale as:  $c_1/c e l_\epsilon$ .



## Large Eddy Simulation (LES)

LES is a numerical method to solve the full, time-dependent Navier-Stokes equations (in their constant-density Boussinesq form) for moment, heat and pollutants, based on parameterisation of the sub-grid scale (SGS) turbulence, see Schumann (Ibid).

LES methods resolves the large scale turbulent motion from first principles by numerically solving a "filtered" set of equations governing this large scale, three-dimensional time dependent motion. Diffusion modelling is here employed only to approximate the effects of the "sub-grid" scale turbulence.

Sub-grid scale turbulence (Reynolds-stresses) are in LES assumed to follow the Kolmogorov (1941) isotropic scaling theory (with energy cascade according to the  $\epsilon^{2/3} k^{-5/3}$  power-law). The dissipation of the corresponding SGS kinetic energy  $\epsilon'' = \frac{1}{2} \langle u''^2 \rangle$  can be parameterized according to Eqs. (42) above.

An important difference relative to the K- $\epsilon$  modelling principle is that the length scale  $l$  here is a fixed quantity and equal to the prescribed grid scale  $\Delta$  (which is typically of the order of 10-100 meters depending on the computer capacity, CPU-time constraints and the stratification).

The sub-grid scale diffusivities (for momentum, heat and pollutants) are also given as above by Eqs.(41), but in terms of the sub-grid kinetic energy  $\epsilon''$  and the associated fixed length scale  $l=\Delta$ .

LES resolves, - in principle at least, in this way the true turbulent atmospheric motion over the range of scales limited by the outer boundary conditions and down to the sub-grid scale  $\Delta$ . Pollutants emitted in this numerical turbulence are advected around explicitly, however, sub-grid pollutant diffusion must also be modelled explicitly: For a continuous (single-particle, ensemble-averaged) releases by use of K-diffusivity in Eqs (41), and for instantaneously released puff's according to Richardson (1926):  $\sigma_p^2 \propto \epsilon T^3$ .

## Large Eddy Simulation Model Equations

Boussinesq equations, constant mean density  $\rho$ :

$$\frac{\partial \bar{u}_j}{\partial x_j} = 0,$$

$$\frac{\partial \bar{u}_i}{\partial t} + \frac{\partial(\bar{u}_j \bar{u}_i)}{\partial x_j} = - \frac{1}{\rho} \frac{\partial \bar{p}}{\partial x_i} - \frac{\partial}{\partial x_j} \overline{u'{}_i u'{}_j} + \beta g_i \bar{T},$$

$$\frac{\partial \bar{T}}{\partial t} + \frac{\partial(\bar{u}_j \bar{T})}{\partial x_j} = - \frac{\partial}{\partial x_j} \overline{u'{}_j T'},$$

and similar for any species concentration  $\psi$ .

Here,

$$\overline{u'{}_i u'{}_j} = \bar{u}_i \bar{u}_j - \bar{u}_j \bar{u}_i$$

are the subgrid-scale (SGS) Reynolds-stresses. The filter denotes the average over a grid volume  
 $V = \Delta x \Delta y \Delta z$ ,

$$\bar{u} = \frac{1}{V} \iiint_V u \, dV,$$

but may also be defined implicitly by the smoothness assumption of the discrete approximation.

If ever possible, one should use isotropic grids, where  $\Delta x = \Delta y = \Delta z$ .

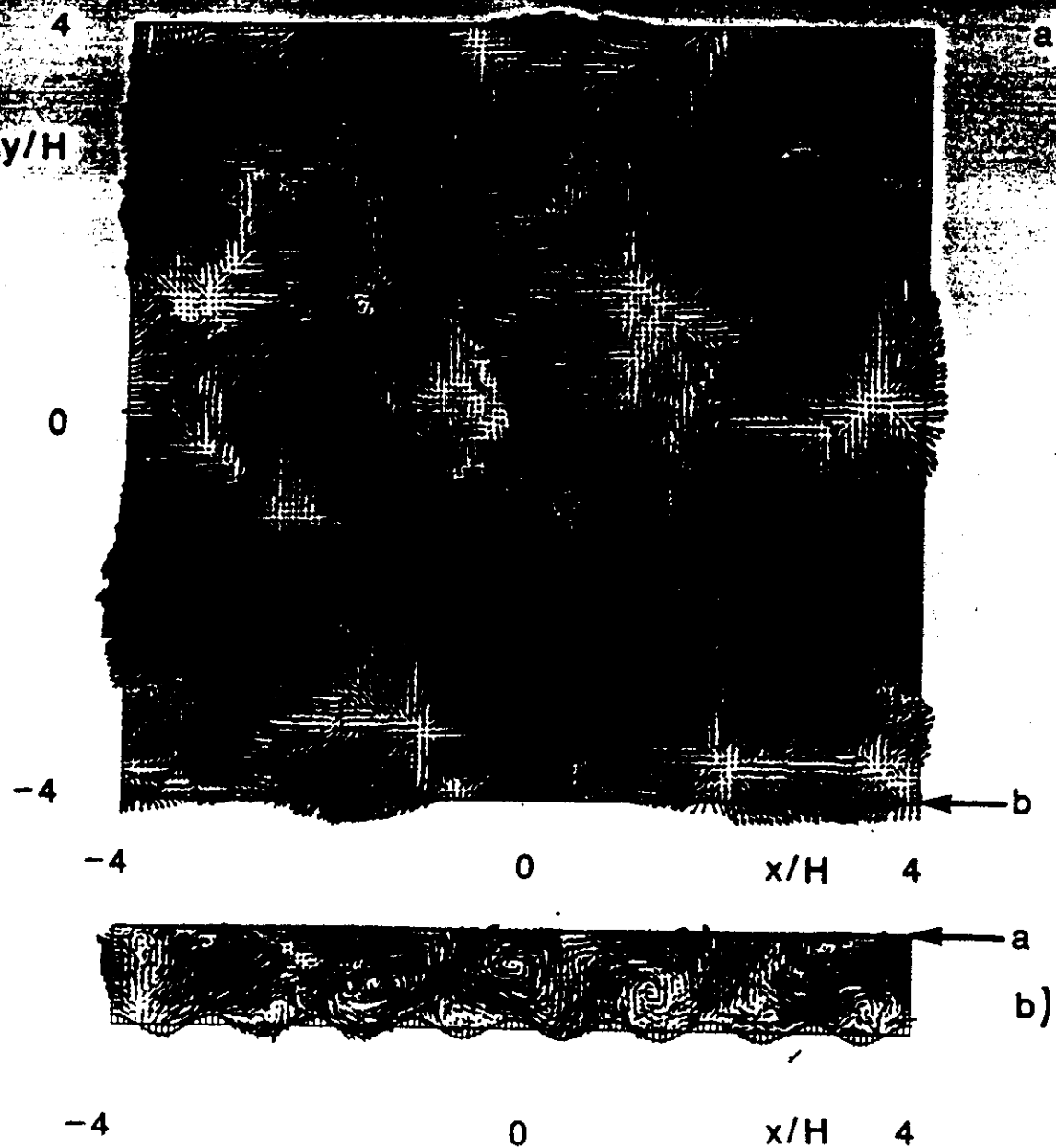
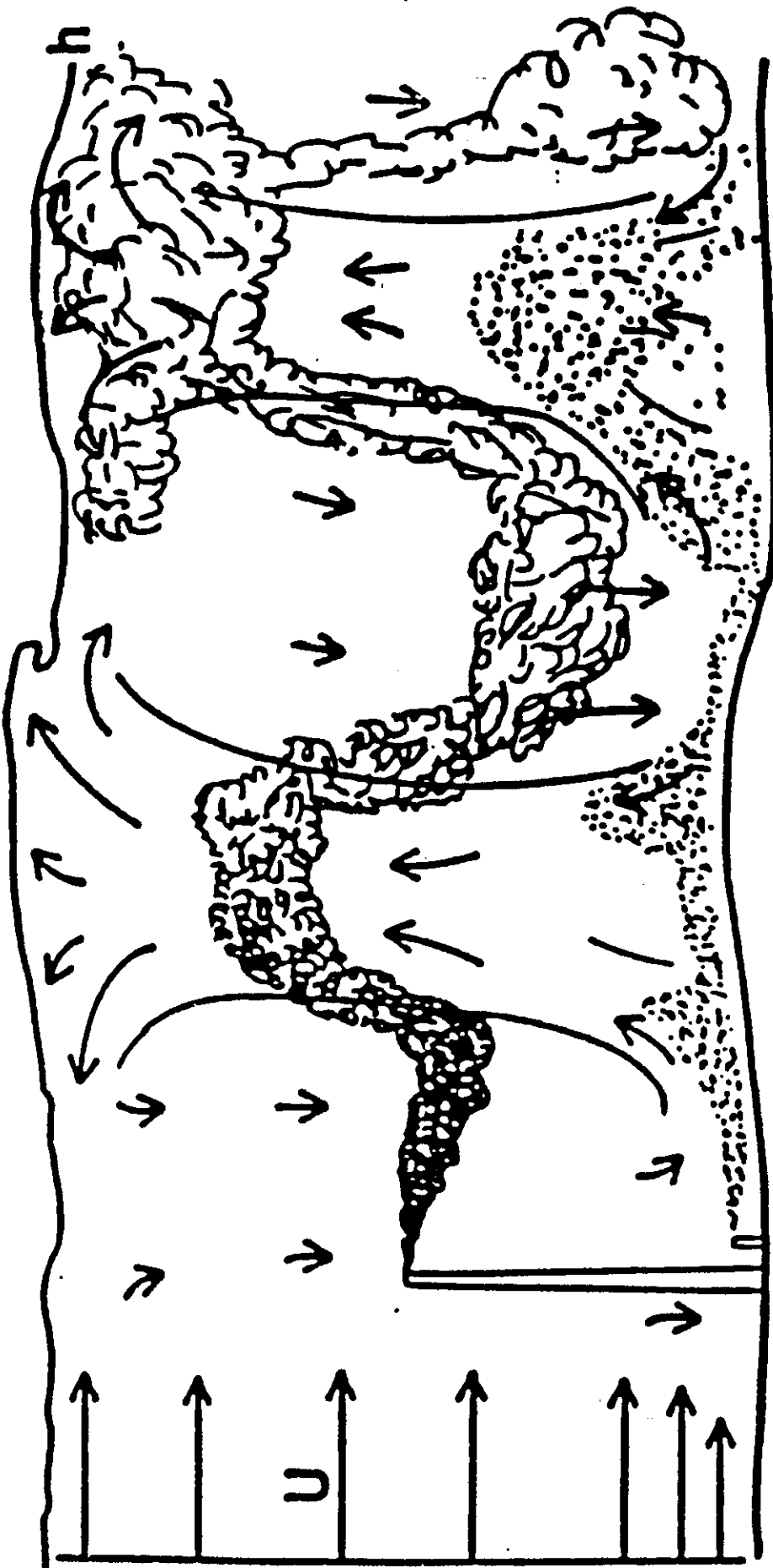
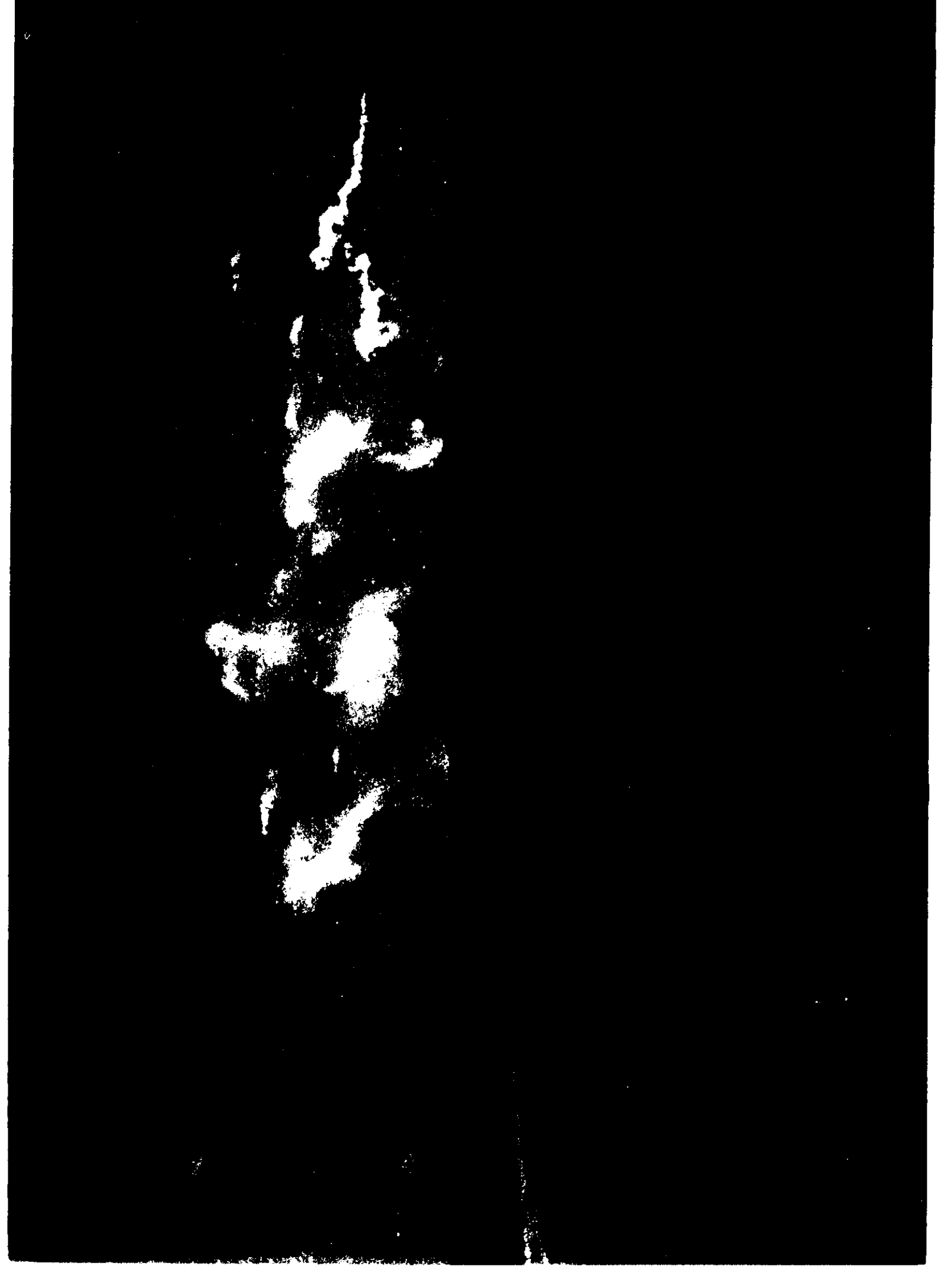


Fig. 9. Velocity vectors, LES over wavy terrain,  $\lambda = H$ ,  $\delta = 0.1$ . a) flow near the upper surface, b) flow in a vertical cross-section near  $y/H = -4$ .

*Schemann.*

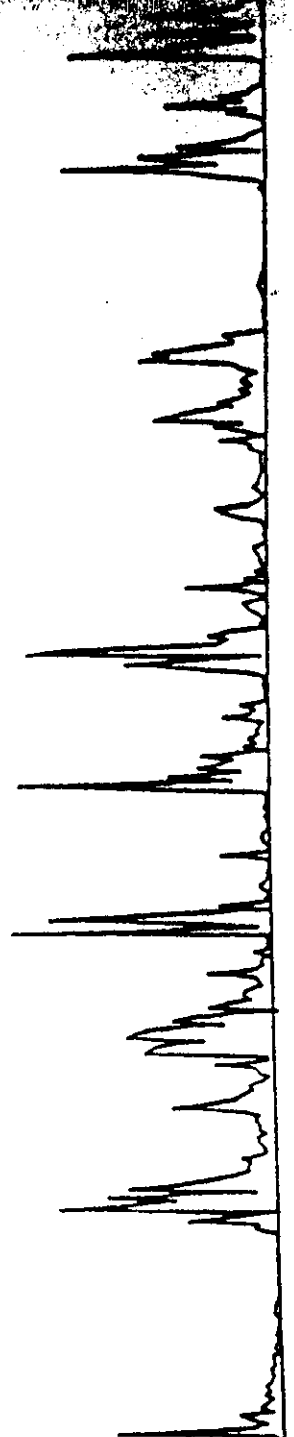




## PART II

### Concentration Fluctuations & LEAD

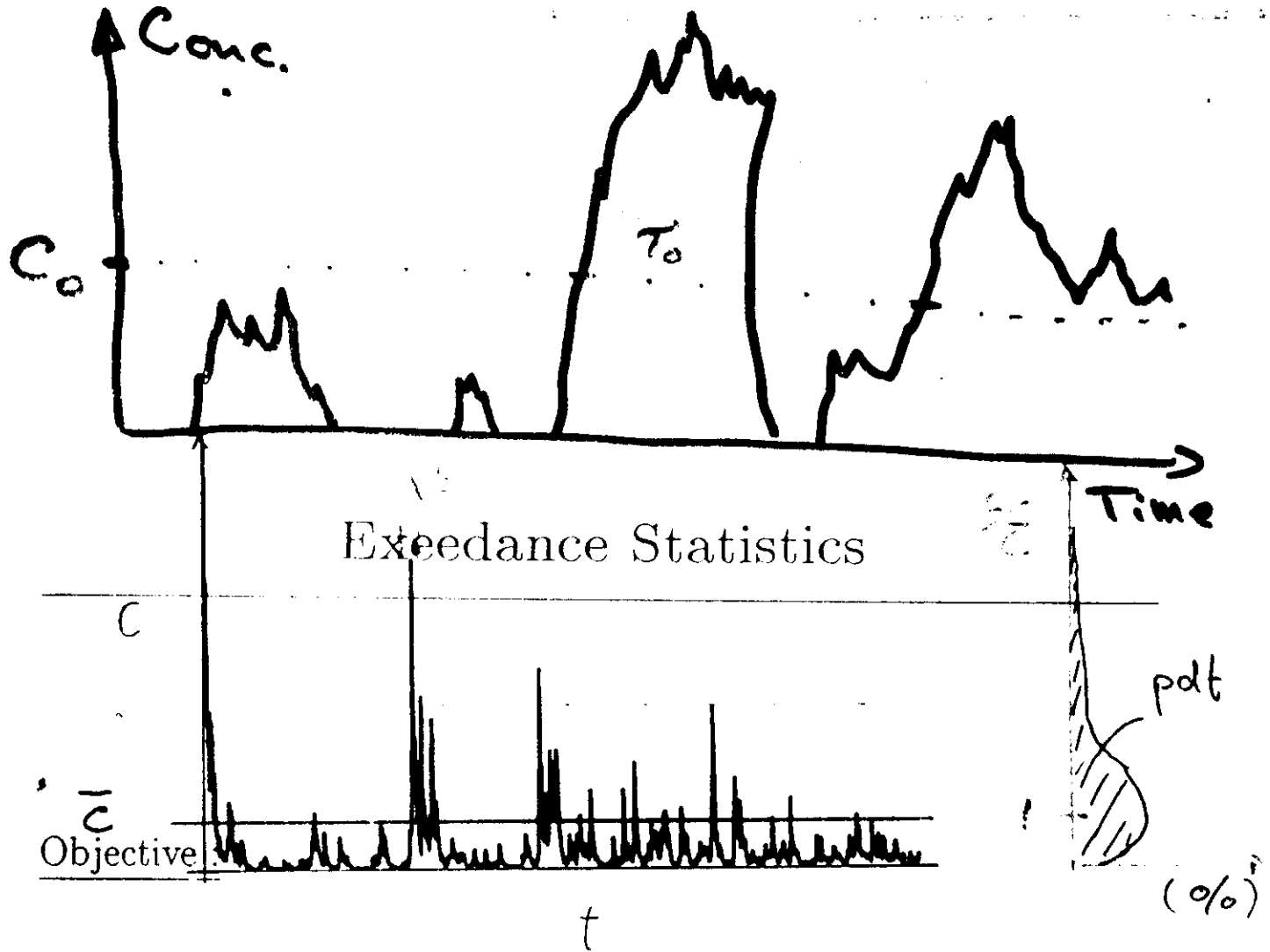
CONCENTRATION



61

Fig. 1. Typical time series measurement of concentrations in a dispersing plume.





- 1: Predict the number of excursions beyond a specified level  $C_0$ .
- 2: Predict the average duration of each excursion beyond the level  $C_0$ .

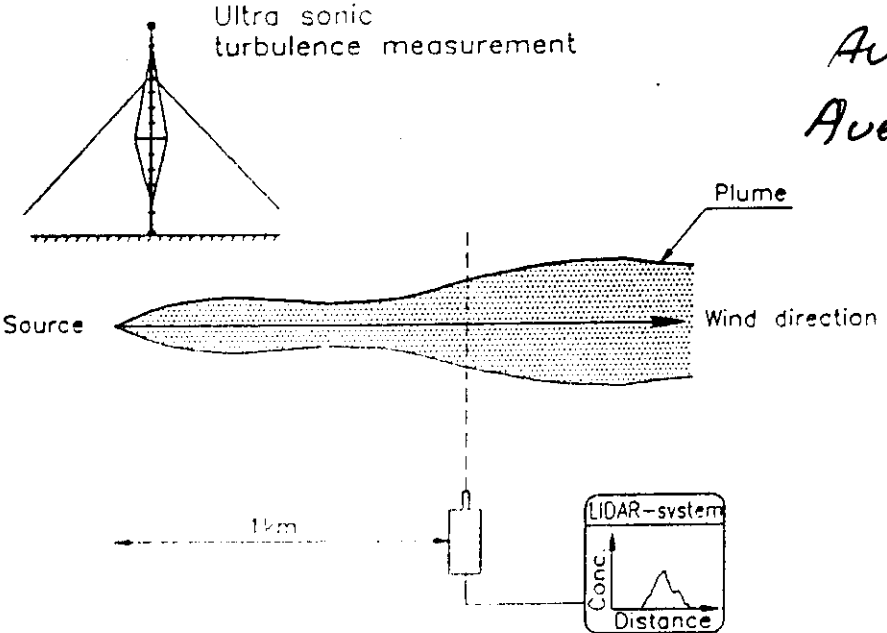


Figure 1. The basic setup in a bird's view for the instruments showing the principal location of the instruments employed

LIDAR - Eqns.

$$P(r) = P_0 A\left(\frac{r}{2}\right) \cdot \frac{\beta(\theta)}{r^2} \cdot e^{-2 \int_0^r \sigma(r') dr'}$$

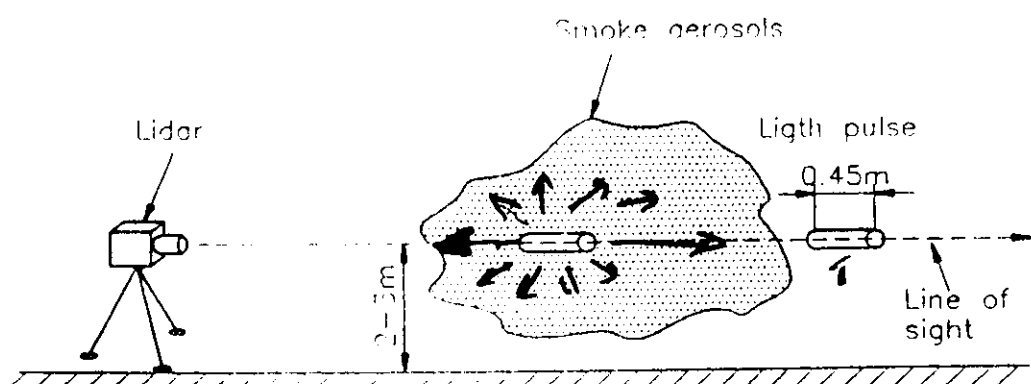
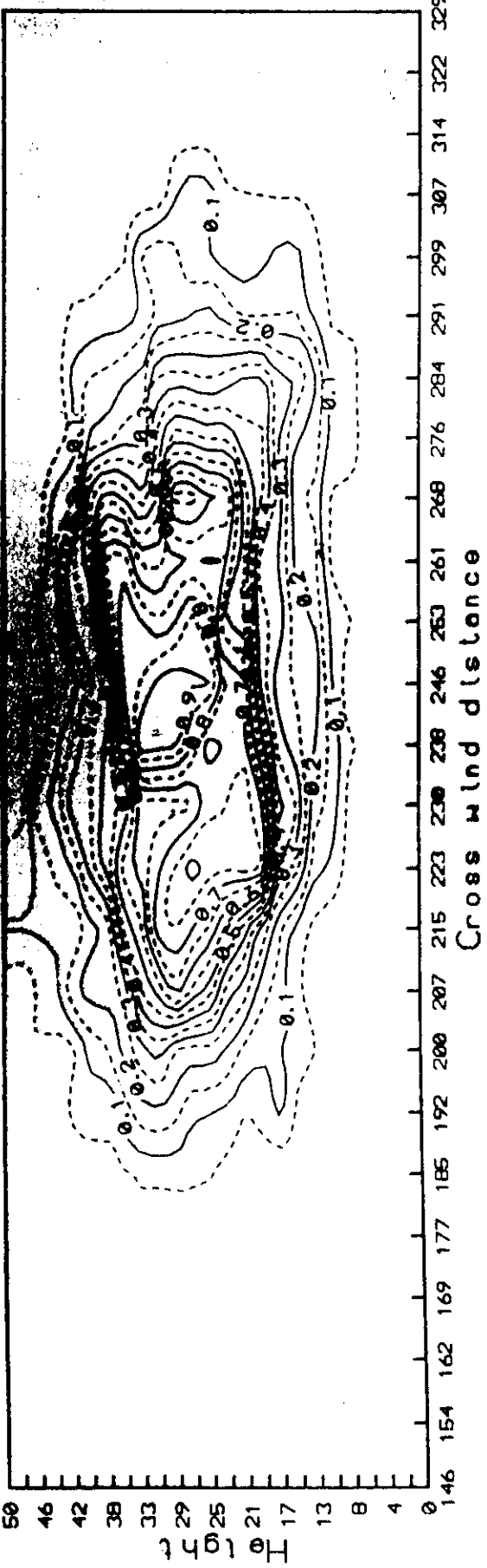
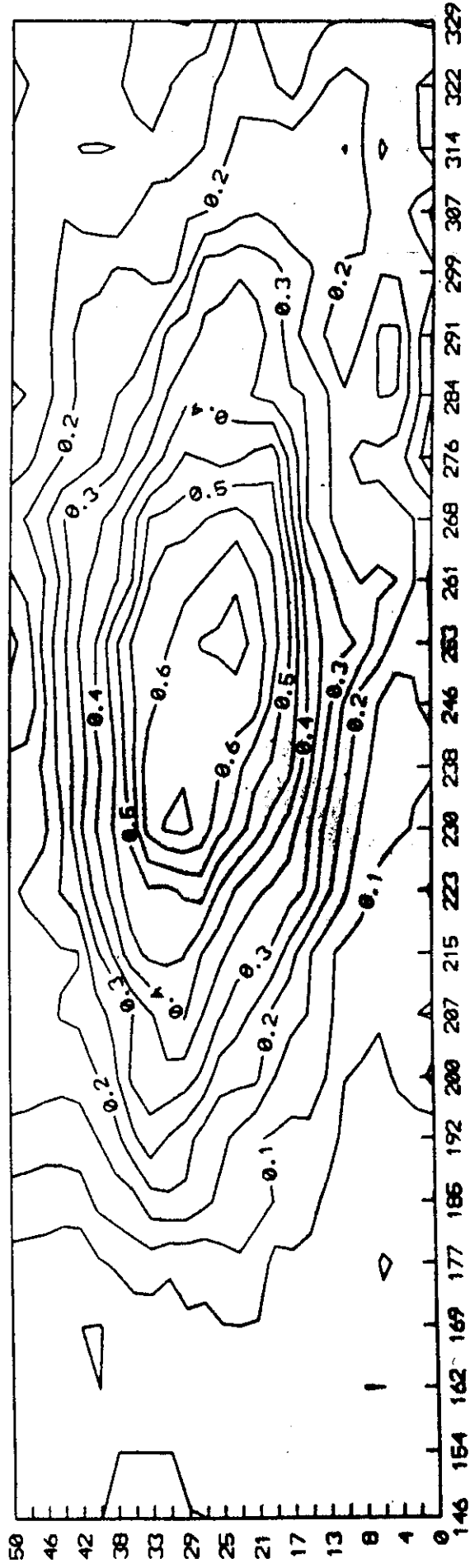


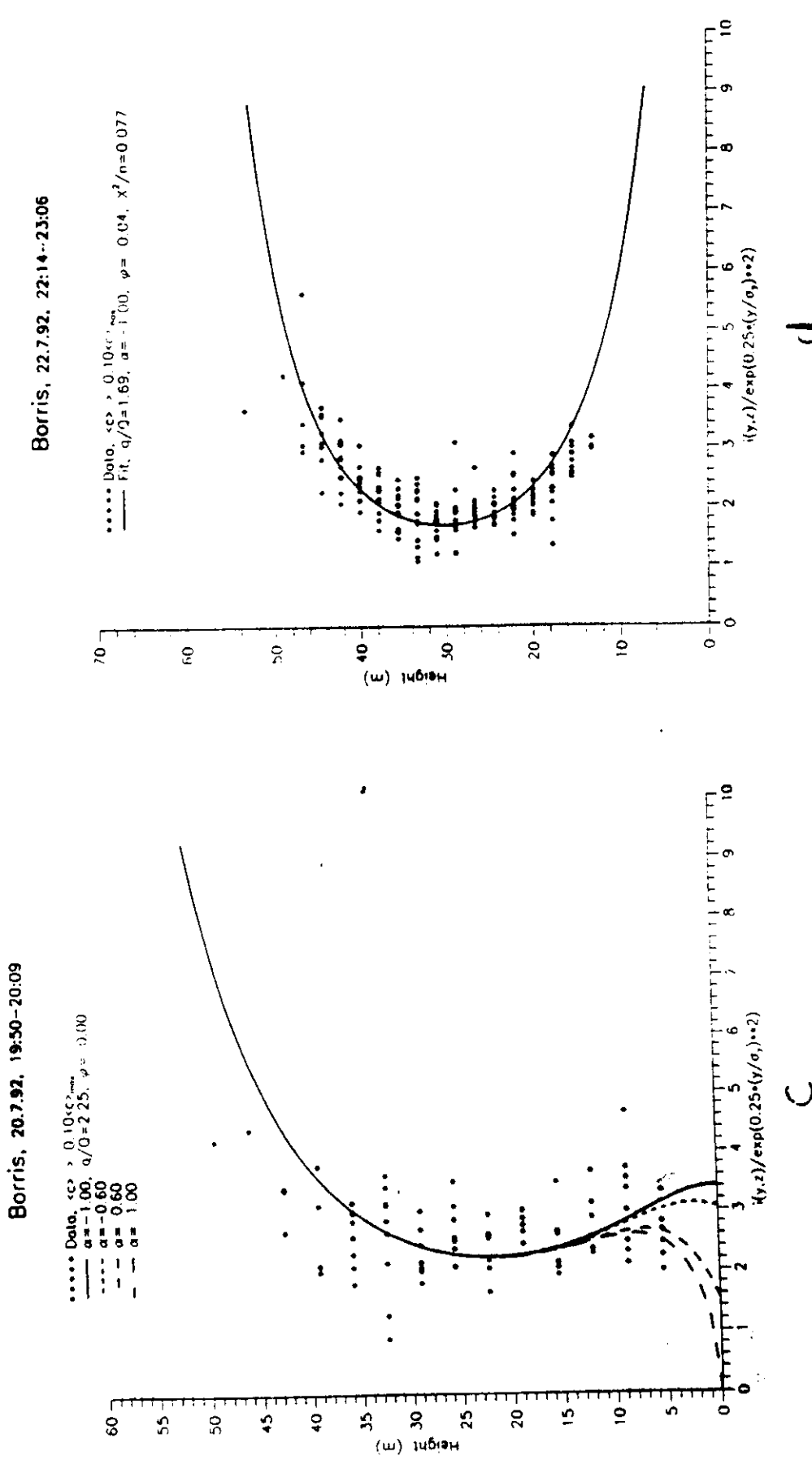
Figure 2. A cross wind section of the plume showing the lidar's line of sight and measuring volume.

# Concentration (%)



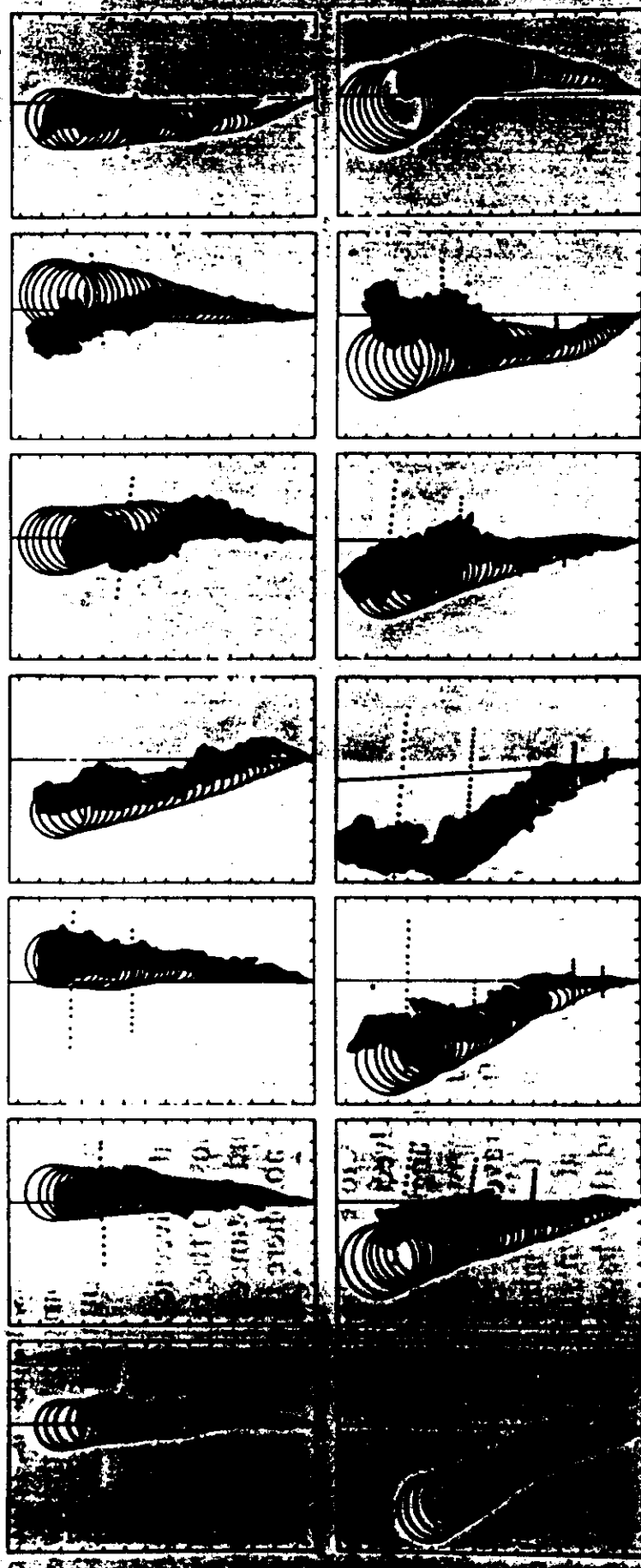
# Intermittency





**Figur 9 c og d.** Eksempler på (fluktuations-) intensiteter målt under eksperimentene i Borris, 20.7.92, 19:30-20:09 og 22.7.92, 22:14-23:06  
**a)** Skan af regfanen som er omtat til vertikale profiler i centerlinien c) under ustabile atmosfæriske forhold i afstanden 300 m og b) under stabile atmosfæriske forhold i afstanden 625 m.

## ARISØ PUFF DIFFUSION MODEL

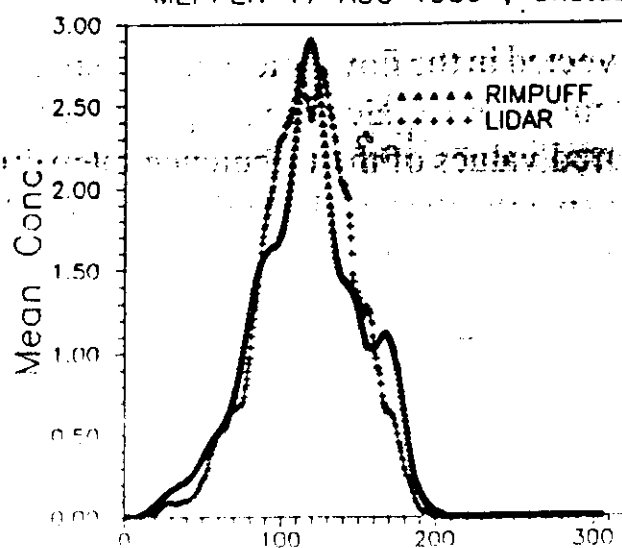


Sequence of 14 instantaneous smoke plume contours (shaded area) obtained from aerial photography during ARISØ RUN 6 experiment. Each picture extends from the source point downwind to  $\sim 500$  m. On top of each contour, the corresponding puff model simulation (circles) of the short-term-averaged smoke plume. The outer radius equals one standard deviation.

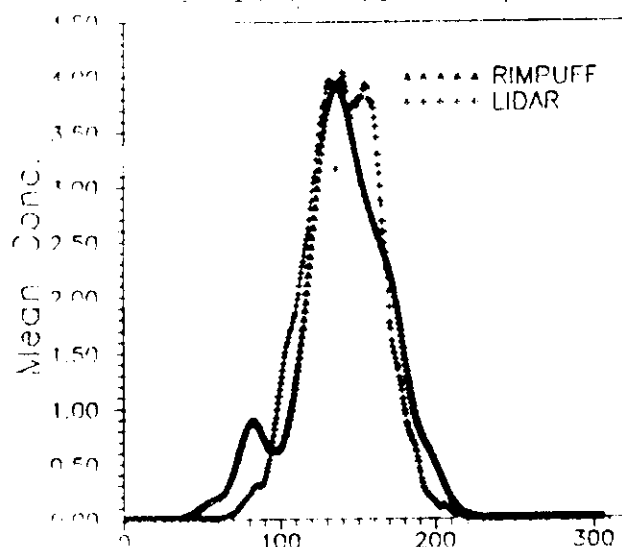
We have also developed interpolation methods which may find useful at greater distances

The puff diffusion model described simulates the release of pollutant puffs and predicts their concentration as they are diffused and advected downwind by

MEPPEN 17 AUG 1989 , Unstable



MEPPEN 17 AUG 1989 , Neutral



MEPPEN 17 AUG 1989 , Stable

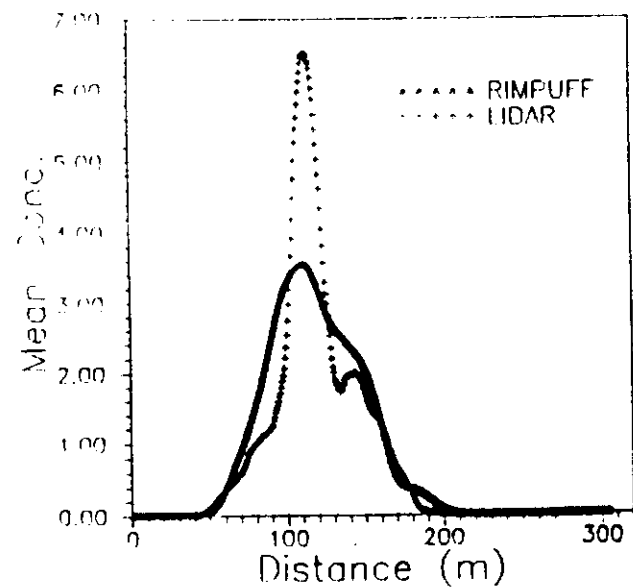


Fig. 8. Modelled and measured mean concentration profile.

## Chemical Rate of Reaction



$$\frac{d[C]}{dt} \propto [A][B]$$

$$[A] = \overline{[A]} + [A]', \quad [B] = \overline{[B]} + [B]'$$

$$\overline{[A]'} = \overline{[B]'} = 0$$

$$\frac{d\overline{[C]}}{dt} \propto \overline{[A]} \overline{[B]} + \overline{[A]'} \overline{[B]}'$$

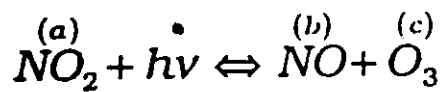
macro micro - mixing  
fluctuations  $\overline{c_i' c_j'}$

Generalized K.  
y.

Intensity of Segregation

$$I_s = \overline{c_i' c_j' / \bar{c}_i \bar{c}_j} \in [-1, 1]$$

# Within the framework of K-theory



$$\frac{\partial a}{\partial t} = -k_2 a + k_1 b.c$$

$$\frac{\partial b}{\partial t} = +k_2 a - k_1 b.c$$

$$\frac{\partial c}{\partial t} = +k_2 a - k_1 b.c$$

yields the following set of equations

$$\overline{wa} = -\overline{w^2} \tau \frac{\partial A}{\partial z} - k_1 \tau (\overline{wb} C + \overline{wc} B) + k_2 \tau \overline{wa}$$

$$\overline{wb} = -\overline{w^2} \tau \frac{\partial B}{\partial z} - k_1 \tau (\overline{wb} C + \overline{wc} B) + k_2 \tau \overline{wa}$$

$$\overline{wc} = -\overline{w^2} \tau \frac{\partial C}{\partial z} + k_1 \tau (\overline{wb} C + \overline{wc} B) - k_2 \tau \overline{wa}$$

which can be rewritten as

$$-\overline{wc_i} = R_y \overline{w^2} \tau \frac{\partial C_j}{\partial z}$$

with

$$R_y = \begin{pmatrix} 1 + k_1 \tau B & k_1 \tau C & -k_2 \tau \\ k_1 \tau B & 1 + k_1 \tau C & -k_2 \tau \\ -k_1 \tau B & -k_1 \tau C & 1 + k_2 \tau \end{pmatrix}$$

$$\text{Continuity eqs} \Rightarrow \left\{ \begin{array}{l} \frac{\partial}{\partial t} + \frac{\partial c_i}{\partial x_j} - \gamma_i \frac{\partial^2 c_i}{\partial x_j^2} \\ = v_i \left( \sum_{m,n}^2 (1 - \delta_{mn}) \frac{k_1}{2} c_m c_n - k_2 c_3 \right) + S_i, \quad i = 1, 2, 3 \end{array} \right. \quad (7)$$

Aux-eqs.

$$\begin{aligned} & \frac{\partial \overline{w' c_i}}{\partial t} + \overline{w'^2} \frac{\partial \overline{c_i}}{\partial z} + \frac{1}{\rho} \left( \overline{c_i} \frac{\partial p}{\partial z} \right) + \frac{\partial \overline{w'^2 c_i}}{\partial z} \\ &= v_i \left( \sum_{m,n}^2 (1 - \delta_{mn}) k_1 \bar{c}_m \overline{w' c_n} - k_2 \overline{w' c_3} \right) \end{aligned} \quad (8)$$

$$\overline{w' c_i} = -K_{ij} \frac{\partial \overline{c_j}}{\partial z} \quad (11)$$

Generalized K

$$K_{ij} = \frac{\kappa u_* (z + z_0)}{1 + r_1 + r_2 + r_3} \begin{pmatrix} 1 + r_1 + r_3 & -r_1 & r_3 \\ -r_2 & 1 + r_2 + r_3 & r_3 \\ r_2 & r_1 & 1 + r_1 + r_3 \end{pmatrix} \quad (12)$$

hvor  $r_i$  er de relevante Damköhlertal givet ved:

$$r_1 = \frac{\tau_t}{\tau_{c1}} = \frac{\kappa(z + z_0) k_1 \overline{NO}}{A u_*} \quad (13)$$

$$r_2 = \frac{\tau_t}{\tau_{c2}} = \frac{\kappa(z + z_0) k_1 \overline{O_3}}{A u_*} \quad (14)$$

$$r_3 = \frac{\tau_t}{\tau_{c3}} = \frac{\kappa(z + z_0) k_2}{A u_*} \quad (15)$$

Kovariansligningen:

$$\begin{aligned} \frac{\partial}{\partial t} \overline{c_i c_j} &= -2 \overline{w' c_i} \frac{\partial \overline{c_j}}{\partial z} - \frac{\partial}{\partial x_l} \overline{w c_i c_j} \\ &+ \gamma_c \frac{\partial^2}{\partial x_l \partial x_l} \overline{c_i c_j} - 2 \gamma_c \frac{\partial \overline{c_i}}{\partial x_l} \frac{\partial \overline{c_j}}{\partial x_l} \\ &+ \sum_{m,n}^2 (1 - \delta_{mn}) k_1 \bar{c}_m (v_j \overline{c_i c_n} + v_i \overline{c_j c_n}) - k_2 (v_j \overline{c_i c_3} + v_i \overline{c_j c_3}) \end{aligned}$$

$$M_{ik} \overline{c_k c_j} = \overline{w' c_i} \frac{\partial \overline{c_j}}{\partial z} + \overline{w' c_j} \frac{\partial \overline{c_i}}{\partial z} \quad (18)$$

hvor  $M_{ik}$  nu er en  $6 \times 6$  matrix i lighed med ligning (13). Ved at invitere matricen  $M_{ik}$  og angive fluxe og midde koncentrationsgradienterne fra løsningen af flux-gradient-ligningerne er man vha. ligning (18) i principippet i stand til at beregne variansudtrykkene:  $\overline{NO'_2}^2$ ,  $\overline{O'_3}^2$ ,  $\overline{NO'_2} \overline{O'_3}$  og kovariansudtrykkene  $\overline{NO' O'_3}$ ,  $\overline{NO' NO'_2}$ ,  $\overline{O'_3 NO'_2}$ .

Macro-mixing

micro-mixing.

